US009605542B2

(12) **United States Patent**
Gallagher et al.

(10) **Patent No.: US 9,605,542 B2**
(45) **Date of Patent: *Mar. 28, 2017**

(54) **GAS TURBINE ENGINE AIRFOIL**

(71) Applicant: **United Technologies Corporation**, Hartford, CT (US)

(72) Inventors: **Edward J. Gallagher**, West Hartford, CT (US); **Byron R. Monzon**, Cromwell, CT (US); **Ling Liu**, Glastonbury, CT (US); **Linda S. Li**, Middlefield, CT (US); **Darryl Whitlow**, Middletown, CT (US); **Barry M. Ford**, Middletown, CT (US)

(73) Assignee: **UNITED TECHNOLOGIES CORPORATION**, Farmington, CT (US)

(*) Notice: Subject to any disclaimer, the term of this patent is extended or adjusted under 35 U.S.C. 154(b) by 63 days.

This patent is subject to a terminal disclaimer.

(21) Appl. No.: **14/624,774**

(22) Filed: **Feb. 18, 2015**

(65) **Prior Publication Data**

US 2015/0354364 A1 Dec. 10, 2015

Related U.S. Application Data

(60) Provisional application No. 61/942,026, filed on Feb. 19, 2014.

(51) **Int. Cl.**
F01D 5/06 (2006.01)
F01D 5/14 (2006.01)

(52) **U.S. Cl.**
CPC ***F01D 5/141*** (2013.01); *F05D 2220/36* (2013.01); *Y02T 50/672* (2013.01); *Y02T 50/673* (2013.01)

(58) **Field of Classification Search**
CPC ... F01D 5/12; F01D 5/14; F01D 5/141; F01D 5/145; F01D 5/06
(Continued)

(56) **References Cited**

U.S. PATENT DOCUMENTS

3,287,906 A 11/1966 McCormick
4,012,172 A 3/1977 Schwaar et al.
(Continued)

FOREIGN PATENT DOCUMENTS

EP 0801230 5/2009
EP 2226468 9/2010
(Continued)

OTHER PUBLICATIONS

Smith, L.,Yeh,H.,(1963).Sweep and Dihedral Effects in Axial-Flow Turbomachinery;Journal of Basic Engineering; Sep. 1963. pp. 401-416.
(Continued)

Primary Examiner — Nathaniel Wiehe
Assistant Examiner — Maxime Adjagbe
(74) *Attorney, Agent, or Firm* — Carlson, Gaskey & Olds, P.C.

(57) **ABSTRACT**

An airfoil for a turbine engine includes an airfoil that has pressure and suction sides that extend in a radial direction from a 0% span position at an inner flow path location to a 100% span position at an airfoil tip. The airfoil has a curve that corresponds to a relationship between a trailing edge sweep angle and a span position. The trailing edge sweep angle is in a range of 10° to 20° in a range of 40-70% span position, and the trailing edge sweep angle is positive from 0% span to at least 95% span. The airfoil has a relationship between a leading edge dihedral and a span position. The leading edge dihedral is negative from the 0% span position to the 100% span position. A positive dihedral corresponds
(Continued)

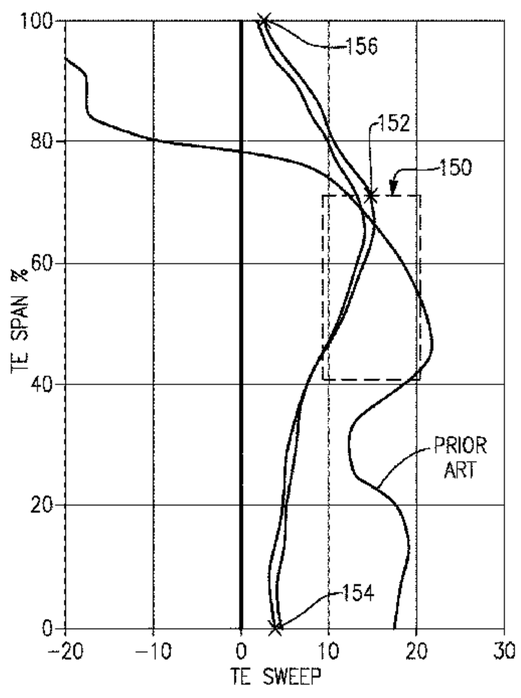

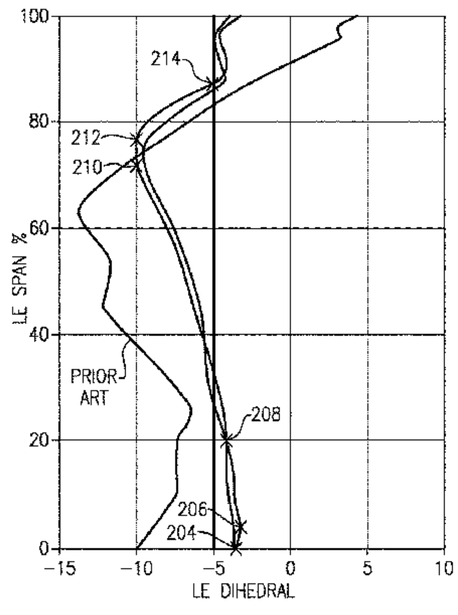

to suction side-leaning, and a negative dihedral corresponds to pressure side-leaning.

30 Claims, 9 Drawing Sheets

(58) **Field of Classification Search**
USPC ..... 416/243, 223 A, DIG. 2, DIG. 5
See application file for complete search history.

(56) **References Cited**

U.S. PATENT DOCUMENTS

4,431,376	A	2/1984	Lubenstein et al.
4,682,935	A	7/1987	Martin
4,826,400	A	5/1989	Gregory
5,088,892	A	2/1992	Weingold et al.
5,141,400	A	8/1992	Murphy et al.
5,167,489	A	12/1992	Wadia et al.
5,443,367	A	8/1995	Samit et al.
5,525,038	A	6/1996	Sharma et al.
5,624,234	A	4/1997	Neely et al.
5,725,354	A	3/1998	Wadia et al.
5,915,917	A	6/1999	Eveker et al.
6,059,532	A	5/2000	Chen et al.
6,079,948	A	6/2000	Sasaki et al.
6,299,412	B1	10/2001	Wood et al.
6,312,219	B1	11/2001	Wood et al.
6,328,533	B1	12/2001	Decker et al.
6,331,100	B1	12/2001	Liu
6,899,526	B2	5/2005	Doloresco et al.
6,994,524	B2	2/2006	Owen et al.
7,204,676	B2	4/2007	Dutton et al.
7,374,403	B2	5/2008	Decker et al.
7,396,205	B2	7/2008	Dube et al.
7,476,086	B2	1/2009	Wadia et al.
7,497,664	B2	3/2009	Walter et al.
7,547,186	B2	6/2009	Schuster et al.
7,806,653	B2	10/2010	Burton et al.
7,997,872	B2	8/2011	Wilson
7,997,882	B2	8/2011	Shulver
8,087,885	B2	1/2012	Suciu et al.
8,147,207	B2	4/2012	Orosa et al.
8,167,567	B2	5/2012	Kirchner et al.
8,246,292	B1	8/2012	Morin et al.
RE43,710	E	10/2012	Spear et al.
8,393,870	B2	3/2013	Nash et al.
8,464,426	B2	6/2013	Kirchner et al.
2003/0086788	A1	5/2003	Chandraker
2003/0163983	A1	9/2003	Seda et al.
2004/0091353	A1	5/2004	Shahpar et al.
2005/0031454	A1	2/2005	Doloresco et al.
2005/0169761	A1	8/2005	Dube et al.
2005/0254956	A1	11/2005	Dutton et al.
2006/0210395	A1	9/2006	Schuster et al.
2006/0228206	A1	10/2006	Decker et al.
2007/0041841	A1	2/2007	Walter et al.
2007/0160478	A1	7/2007	Jarrah et al.
2007/0201983	A1	8/2007	Arinci et al.
2007/0243068	A1	10/2007	Wadia et al.
2008/0101959	A1	5/2008	McRae et al.
2008/0120839	A1	5/2008	Schilling
2008/0148564	A1	6/2008	Burton et al.
2008/0226454	A1	9/2008	Decker et al.
2009/0226322	A1	9/2009	Clemen
2009/0274554	A1	11/2009	Guemmer
2009/0304518	A1	12/2009	Kodama et al.
2009/0317227	A1	12/2009	Grover et al.
2010/0054946	A1	3/2010	Orosa et al.
2010/0148396	A1	6/2010	Xie et al.
2010/0232970	A1	9/2010	Murooka et al.
2010/0254797	A1	10/2010	Grover et al.
2010/0260609	A1	10/2010	Wood et al.
2010/0331139	A1	12/2010	McCune
2011/0081252	A1	4/2011	Li
2011/0135482	A1	6/2011	Nash et al.
2011/0206527	A1	8/2011	Harvey et al.
2011/0225979	A1	9/2011	Hoeger et al.
2011/0268578	A1	11/2011	Praisner et al.
2011/0286850	A1	11/2011	Micheli et al.
2012/0057982	A1	3/2012	O'Hearn et al.
2012/0195767	A1	8/2012	Gervais et al.
2012/0237344	A1	9/2012	Wood et al.
2012/0243975	A1	9/2012	Breeze-Stringfellow et al.
2012/0244005	A1	9/2012	Breeze-Stringfellow et al.
2013/0008170	A1	1/2013	Gallagher et al.
2013/0022473	A1	1/2013	Tran
2013/0089415	A1	4/2013	Brown et al.
2013/0149108	A1	6/2013	Webster
2013/0164488	A1	6/2013	Wood et al.
2013/0189117	A1	7/2013	Baltas et al.
2013/0202403	A1	8/2013	Morin et al.
2013/0219922	A1	8/2013	Gilson et al.
2013/0224040	A1	8/2013	Straccia
2013/0266451	A1	10/2013	Pesteil et al.
2013/0340406	A1	12/2013	Gallagher et al.
2014/0030060	A1	1/2014	Magowan
2014/0248155	A1*	9/2014	Merville et al. ..... 416/223 R
2015/0354367	A1	12/2015	Gallagher et al.

FOREIGN PATENT DOCUMENTS

EP	2535527	12/2012
EP	2543818	1/2013
GB	1516041	6/1978
GB	2041090	9/1980
WO	2007038674	4/2007

OTHER PUBLICATIONS

Engine Specifications. Engine Alliance GP7200—The Engine for the A380. Retrieved Feb. 19, 2015 from http://www.enginealliance.com/engine_specifications.html.

Conference on Engineering and Physics: Synergy for Success 2006. Journal of Physics: Conference Series vol. 105. London, UK. Oct. 5, 2006.

Kurzke, J. (2009). Fundamental differences between conventional and geared turbofans. Proceedings of ASME Turbo Expo: Power for Land, Sea, and Air. 2009, Orlando, Florida.

Agarwal, B.D and Broutman, L.J. (1990). Analysis and performance of fiber composites, 2nd Edition. John Kiley & Sons, Inc. New York: New York.

Carney, K., Pereira, M. Revilock, and Matheny, P. Jet engine fan blade containment using two alternate jeometries. 4th European LS-DYNA Users Conference.

Brines, G.L. (1990). The turbofan of tomorrow. Mechanical Engineering: the Journal of the American Society of Mechanical Engineers,108(8), 65-67.

Faghri, A. (1995). Heat pipe and science technology. Washington, D.C.: Taylor & Francis.

Hess, C. (1998). Pratt & Whitney develops geared turbofan. Flug Revue 43(7). Oct. 1998.

Grady, J.E., Weir, D.S., Lamoureux, M.C., and Martinez, M.M. (2007). Engine noise research in NASA's quiet aircraft technology project. Papers from the International Symposium on Air Breathing Engines (ISABE). 2007.

Griffiths, B. (2005). Composite fan blade containment case. Modem Machine Shop. Retrieved from: http://www.mimsonline.com/articles/composite-fan-blade-containment-case.

Hall, C.A. And Crichton, D. (2007). Engine design studies for a silent aircraft. Journal of Turbomachinery, 129, 479-487.

Haque, A. and Shamsuzzoha, M., Hussain, F., and Dean, D. (2003). S20-glass/epoxy polymer nanocomposites: Manufacturing, structures, thermal and mechanical properties. Journal of Composite Materials, 37 (20), 1821-1837.

Brennan, P.J. and Kroliczek, E.J. (1979). Heat pipe design handbook. Prepared for National Aeronautics and Space Administration by B & K Engineering, Inc. Jun. 1979.

Horikoshi, S. and Serpone, N. (2013). Introduction to nanoparticles. Microwaves in nanoparticle synthesis. Wiley-VCH Verlag GmbH & Co. KGaA.

(56) **References Cited**

OTHER PUBLICATIONS

Kerrebrock, J.L. (1977). Aircraft engines and gas turbines. Cambridge, MA: The MIT Press.
Xie, M. (2008). Intelligent engine systems: Smart case system. NASA/CR-2008-215233.
Knip, Jr., G. (1987). Analysis of an advanced technology subsonic turbofan incorporating revolutionary materials. NASA Technical Memorandum. May 1987.
Willis, W.S. (1979). Quiet clean short-haul experimental engine (QCSEE) final report NASA/CR-159473.
Kojima, Y., Usuki, A. Kawasumi, M., Okada, A., Fukushim, Y., Kurauchi, T., and Kamigaito, O. (1992). Mechanical properties of nylon 6-clay hybrid. Journal of Materials Research, 8(5), 1185-1189.
Kollar, L.P. and Springer, G.S. (2003). Mechanics of composite structures. Cambridge, UK: Cambridge University Press.
Ramsden, J.M. (Ed). (1978). The new European airliner. Flight International, 113(3590). Jan. 7, 1978.
Langston, L. and Faghri, A. Heat pipe turbine vane cooling. Prepared for Advanced Turbine Systems Annual Program Review. Morgantown, West Virginia. Oct. 17-19, 1995.
Oates, G.C. (Ed). (1989). Aircraft propulsion systems and technology and design. Washington, D.C.: American Institute of Aeronautics, Inc.
Lau, K, Gu, C., and Hui, D. (2005). A critical review on nanotube and nanotube/nanoclay related polymer composite materials. Composites: Part B 37(2006) 425-436.
Shorter Oxford English dictionary, fith Edition. (2007). vol. 2, N-Z. p. 1888.
Lynwander, P. (1983). Gear drive systems: Design and application. New York, New York: Marcel Dekker, Inc.
Sweetman, B. and Sutton, O. (1998). Pratt & Whitney's surprise leap. Interavia Business & Technology, 53.621, p. 25.
Mattingly, J.D. (1996). Elements of gas turbine propulsion. New York, New York: McGraw-Hill, Inc.
Pyrograf-III Carbon Nanofiber. Product guide. Retrieved from: http://pyrografproducts.com/Merchant5/merchant.
mvc?Screen=cp_nanofiber.
Nanocor Technical Data for Epoxy Nanocomposites using Nanomer 1.30E Nanoclay. Nnacor, Inc.
Ratna, D. (2009). Handbook of thermoset resins. Shawbury, UK: iSmithers.
Wendus, B.E., Stark, D.F., Holler, R.P., and Funkhouser, M.E. (2003). Follow-on technology requirement study for advanced subsonic transport. NASA/CR-2003-212467.
Silverstein, C.C., Gottschlich, J.M., and Meininger, M. The feasibility of heat pipe turbine vane cooling. Presented at the International Gas Turbine and Aeroengine Congress and Exposition, The Hague, Netherlands. Jun. 13-16, 1994.
Merriam-Webster's collegiate dictionary, 11th Ed. (2009). p. 824.
Merriam-Webster's collegiate dictionary, 10th Ed. (2001). p. 1125-1126.
Whitaker, R. (1982). ALF502: plugging the turbofan gap. Flight International, p. 237-241, Jan. 30, 1982.
Hughes, C. (2010). Geared turbofan technology. NASA Environmentally Responsible Aviation Project. Green Aviation Summit. NASA Ames Research Center. Sep. 8-9, 2010.
The International Search Report and Written Opinion for PCT Application No. PCT/US2015/016083, mailed Jul. 21, 2015.
The International Search Report and Written Opinion for PCT Application No. PCT/US2015/016187, mailed May 20, 2015.
The International Search Report and Written Opinion for PCT Application No. PCT/US2015/016011, mailed May 21, 2015.
The International Search Report and Written Opinion for PCT Application No. PCT/US2015/016078, mailed May 29, 2015.
The International Search Report and Written Opinion for PCT Application No. PCT/US2015/016154, mailed May 22, 2015.
The International Search Report and Written Opinion for PCT Application No. PCT/US2015/016086, mailed May 26, 2015.
The International Search Report and Written Opinion for PCT Application No. PCT/US2015/016554, mailed May 26, 2015.
The International Search Report and Written Opinion for PCT Application No. PCT/US2015/015554, mailed May 21, 2015.
The International Search Report and Written Opinion for PCT Application No. PCT/US2014/052325, mailed May 29, 2015.
The International Search Report and Written Opinion for PCT Application No. PCT/US2015/016378, mailed May 29, 2015.
The International Search Report and Written Opinion for PCT Application No. PCT/US2014/052293, mailed May 29, 2015.
The International Search Report and Written Opinion for PCT Application No. PCT/US2014/052516, mailed Jun. 10, 2015.
Aerodynamic Design technique for Optimizing Fan Blade Spacing, Rogalsky et all., Proceedings of the 7th Annual Conference of the Computational Fluid Dynamics Society of Canada, 1999.
Turbine Design and Application. vol. 2. NASA, 1973.
Analytical Parametric Investigation of Low Pressure Ration Fan, NASA, 1973 Metzger et al.
Oyama et al., Multiobjective Optimization of a Multi-Stage Compressor Using Evolutionary Algorithm, NASA, 2002, AIAA 2002-3535 pp. 1-11.
International Search Report and Written Opinion for PCT Application No. PCT/US2015/016018, mailed Nov. 24, 2015.
International Search Report and Written Opinion for PCT Application No. PCT/US2015016091, mailed Nov. 24, 2015.
International Search Report and Written Opinion for PCT Application No. PCT/US2015/016032, mailed Nov. 24, 2015.
International Search Report and Written Opinion for PCT Application No. PCT/US2015/016135, mailed Nov. 24, 2015.
International Search Report and Written Opinion for PCT Application No. PCT/US2015/016584, mailed Nov. 24, 2015.
International Search Report and Written Opinion for PCT Application No. PCT/US2015/015561, mailed Nov. 24, 2015.
International Search Report and Written Opinion for PCT Application No. PCT/US2015/015575, mailed Nov. 24, 2015.
International Search Report and Written Opinion for PCT Application No. PCT/US2015/015579, mailed Nov. 24, 2015.
International Search Report and Written Opinion for PCT Application No. PCT/US2015/015586, mailed Nov. 24, 2015.
International Preliminary Report on Patentability for PCT Application No. PCT/US2014/052282, mailed Sep. 1, 2016.
International Preliminary Report on Patentability for PCT Application No. PCT/US2015/016554, mailed Sep. 1, 2016.
International Preliminary Report on Patentability for PCT Application No. PCT/US2014/052434, mailed Sep. 1, 2016.
International Preliminary Report on Patentability for PCT Application No. PCT/US2014/052516, mailed Sep. 1, 2016.
International Preliminary Report on Patentability for PCT Application No. PCT/US2014/052447, mailed Sep. 1, 2016.
International Preliminary Report on Patentability for PCT Application No. PCT/US2015/015579, mailed Sep. 1, 2016.
International Preliminary Report on Patentability for PCT Application No. PCT/US2015/015586, mailed Sep. 1, 2016.
International Preliminary Report on Patentability for PCT Application No. PCT/US2014/052080, mailed Sep. 1, 2016.
International Preliminary Report on Patentability for PCT Application No. PCT/US2015/016135, mailed Sep. 1, 2016.
International Preliminary Report on Patentability for PCT Application No. PCT/US2015/016032 mailed Sep. 1, 2016.
International Preliminary Report on Patentability for PCT Application No. PCT/US2015/015561 mailed Sep. 1, 2016.

* cited by examiner

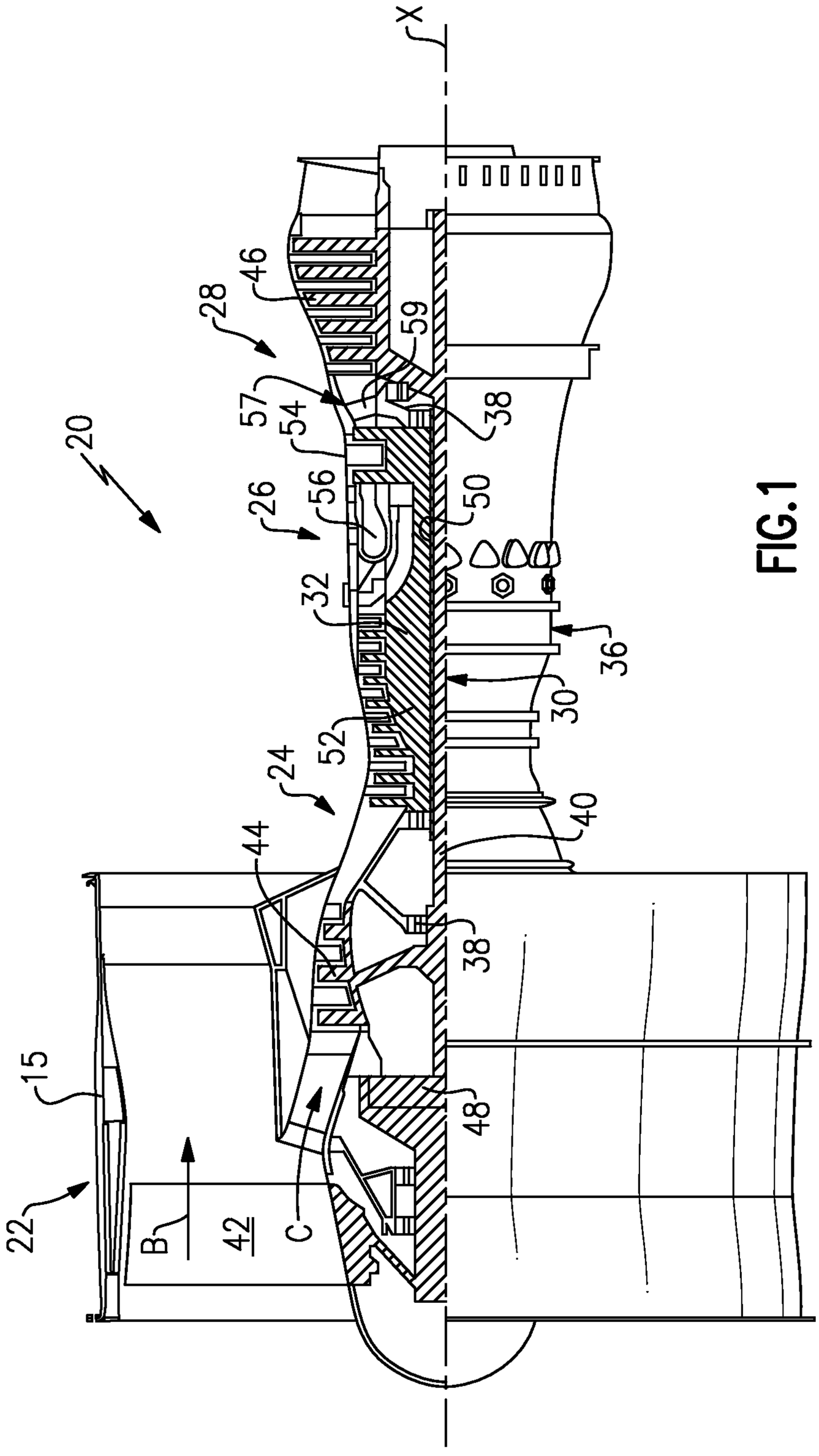

FIG.1

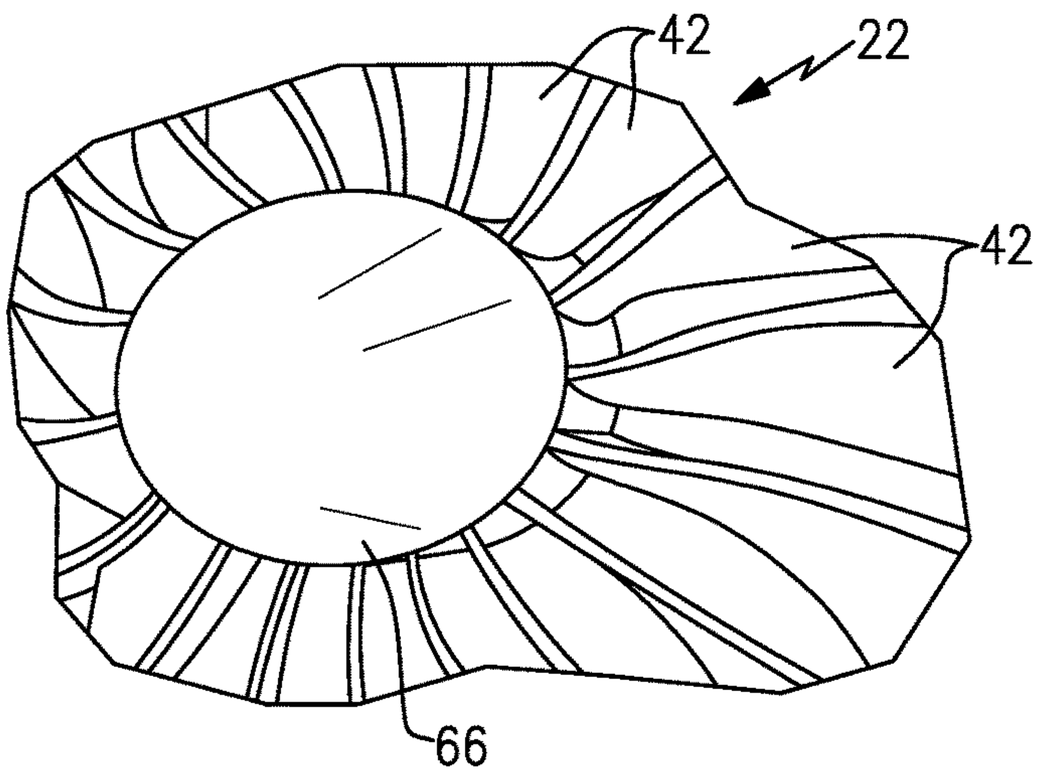

FIG.2A

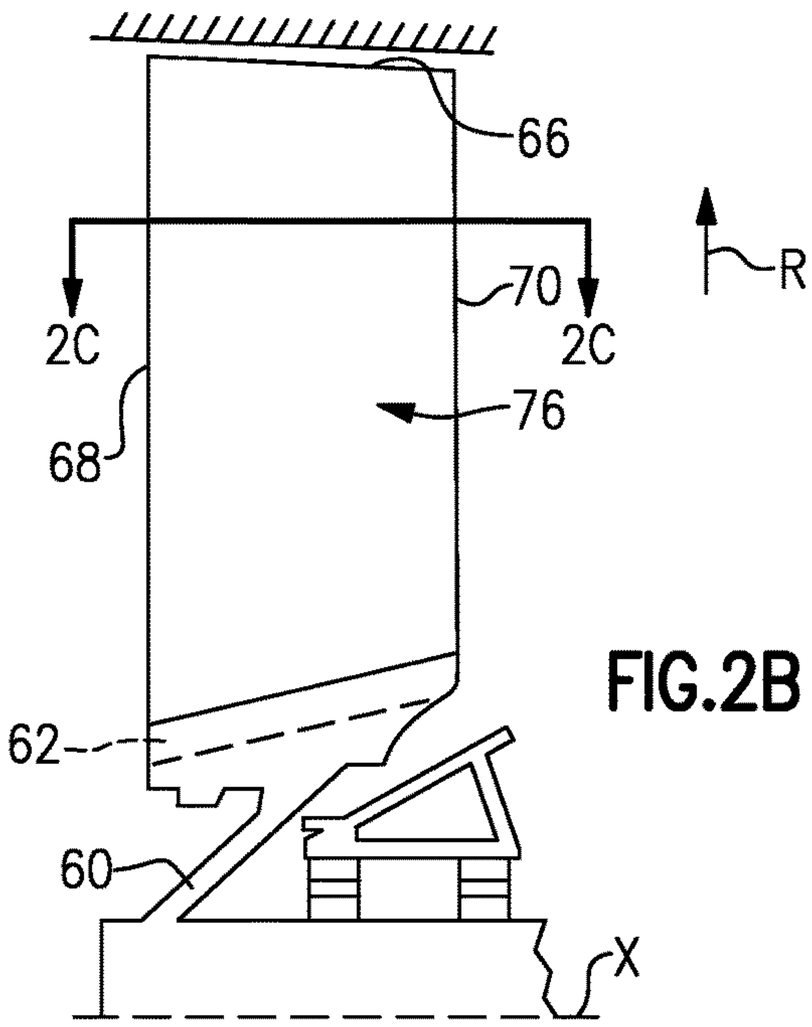

FIG.2B

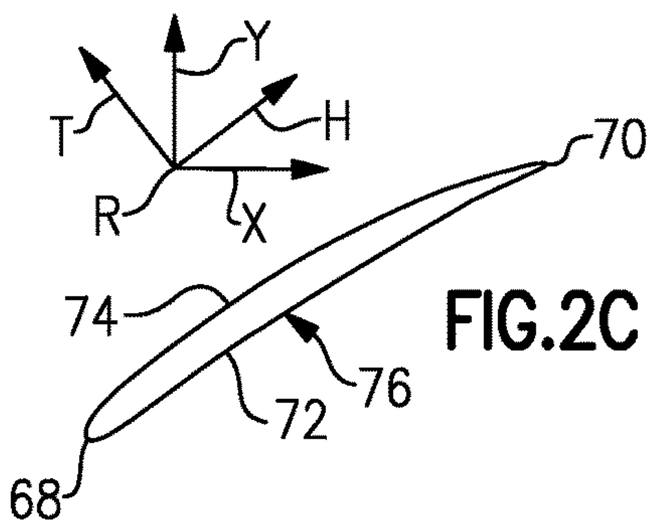

FIG.2C

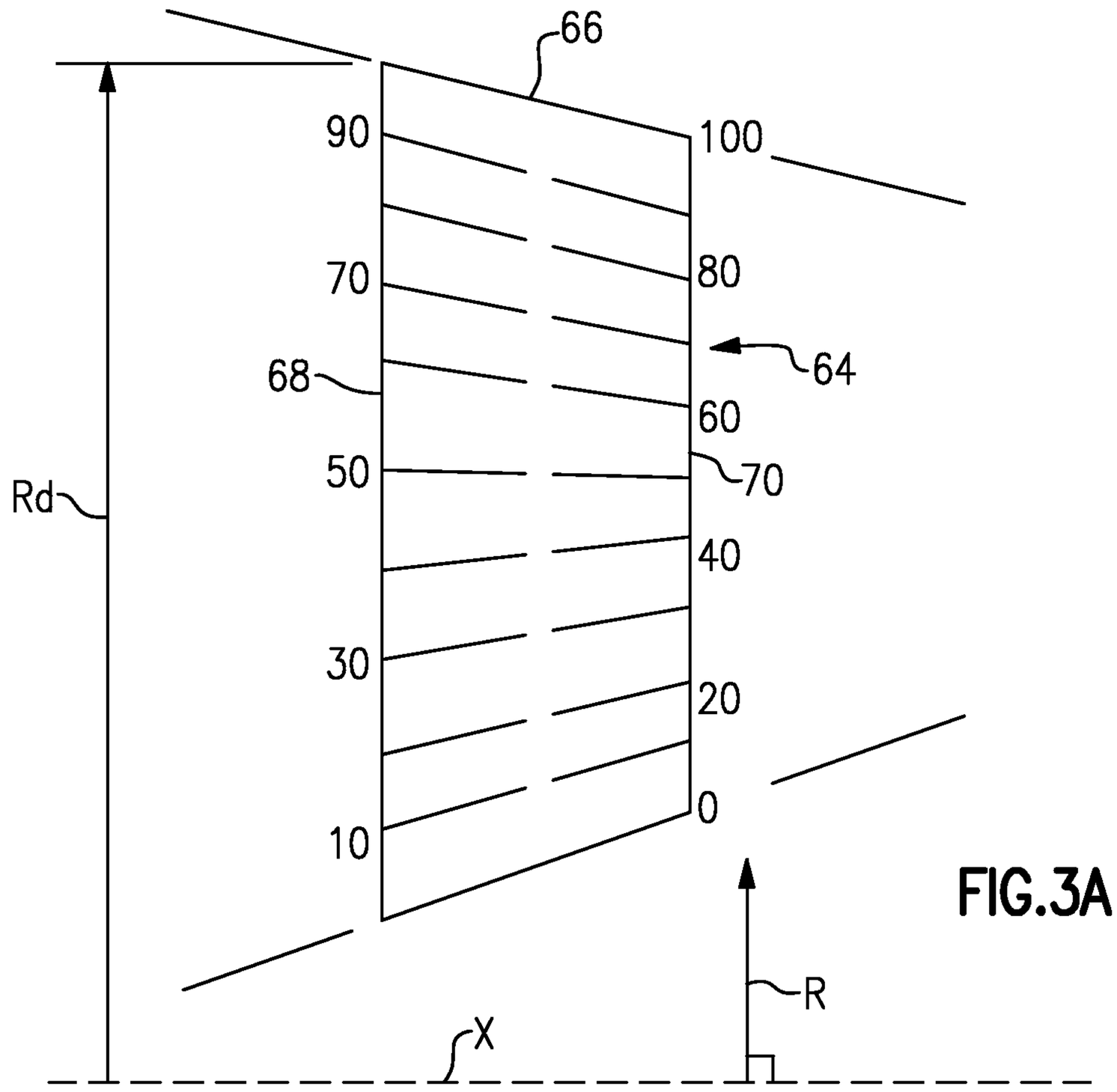
66
90
100
70
80
68
64
60
50
70
Rd
40
30
20
10
0
R
X

FIG.3A

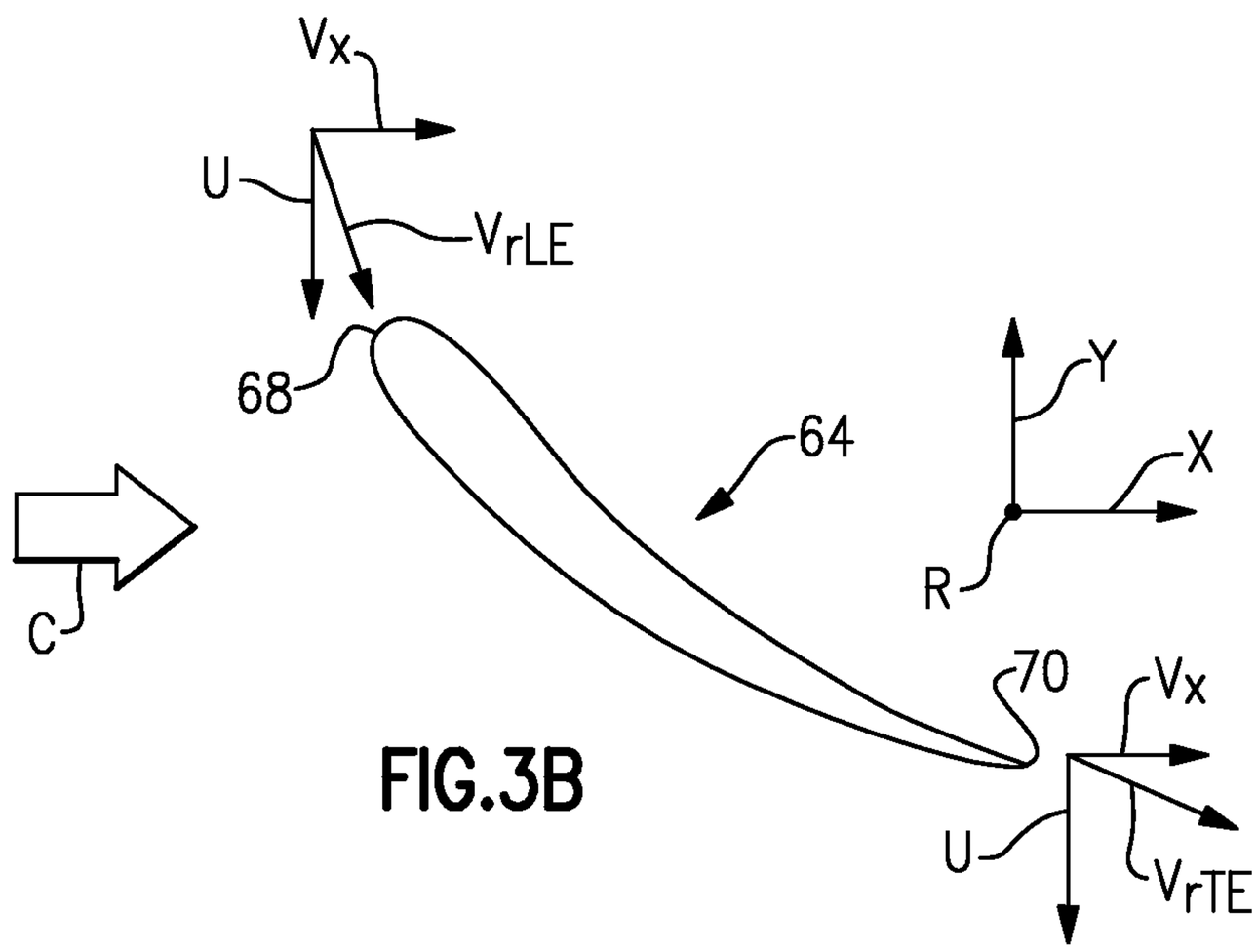
Vx
U
VrLE
68
64
Y
X
R
C
70
Vx
U
VrTE

FIG.3B

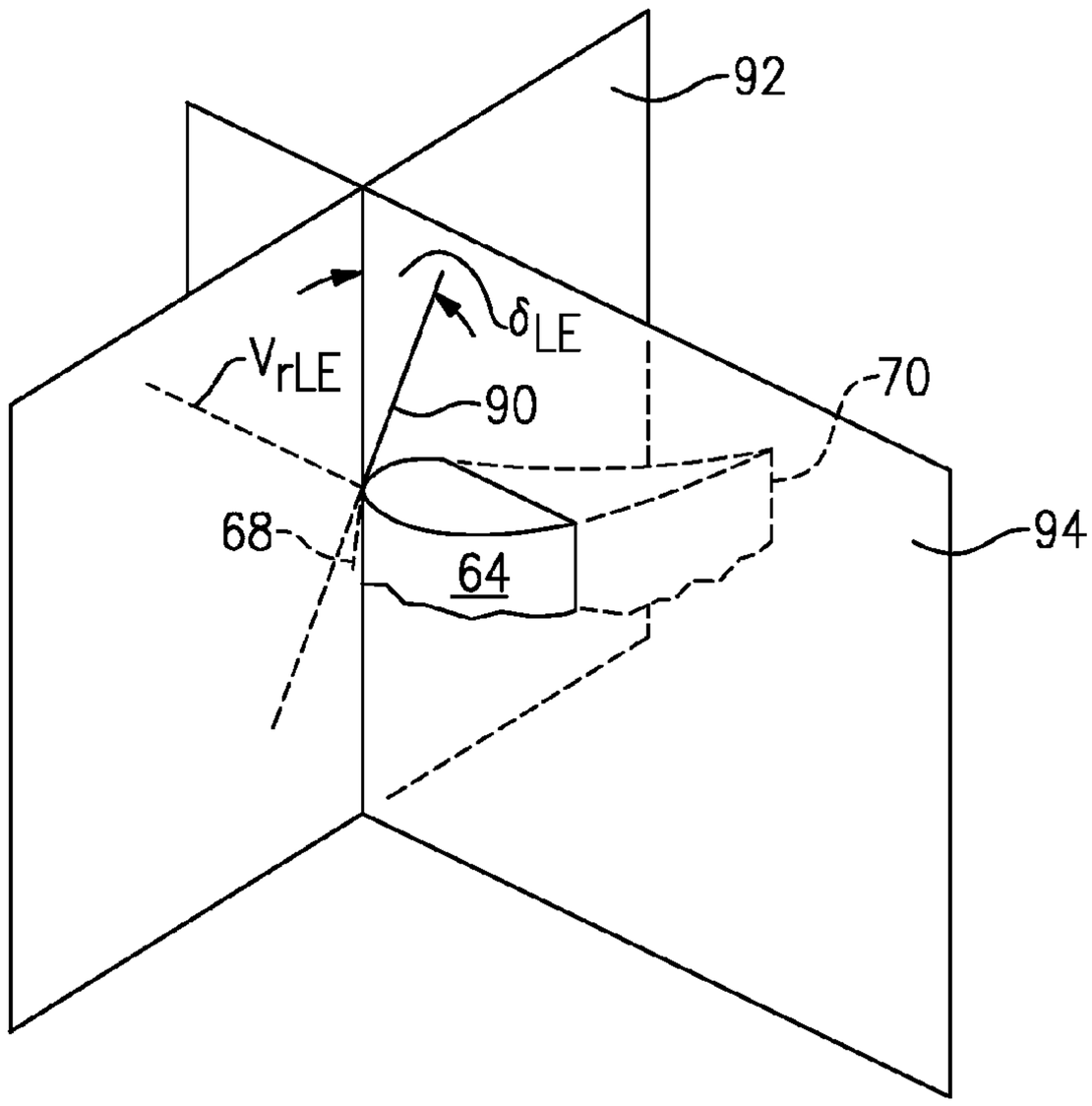

FIG.3C

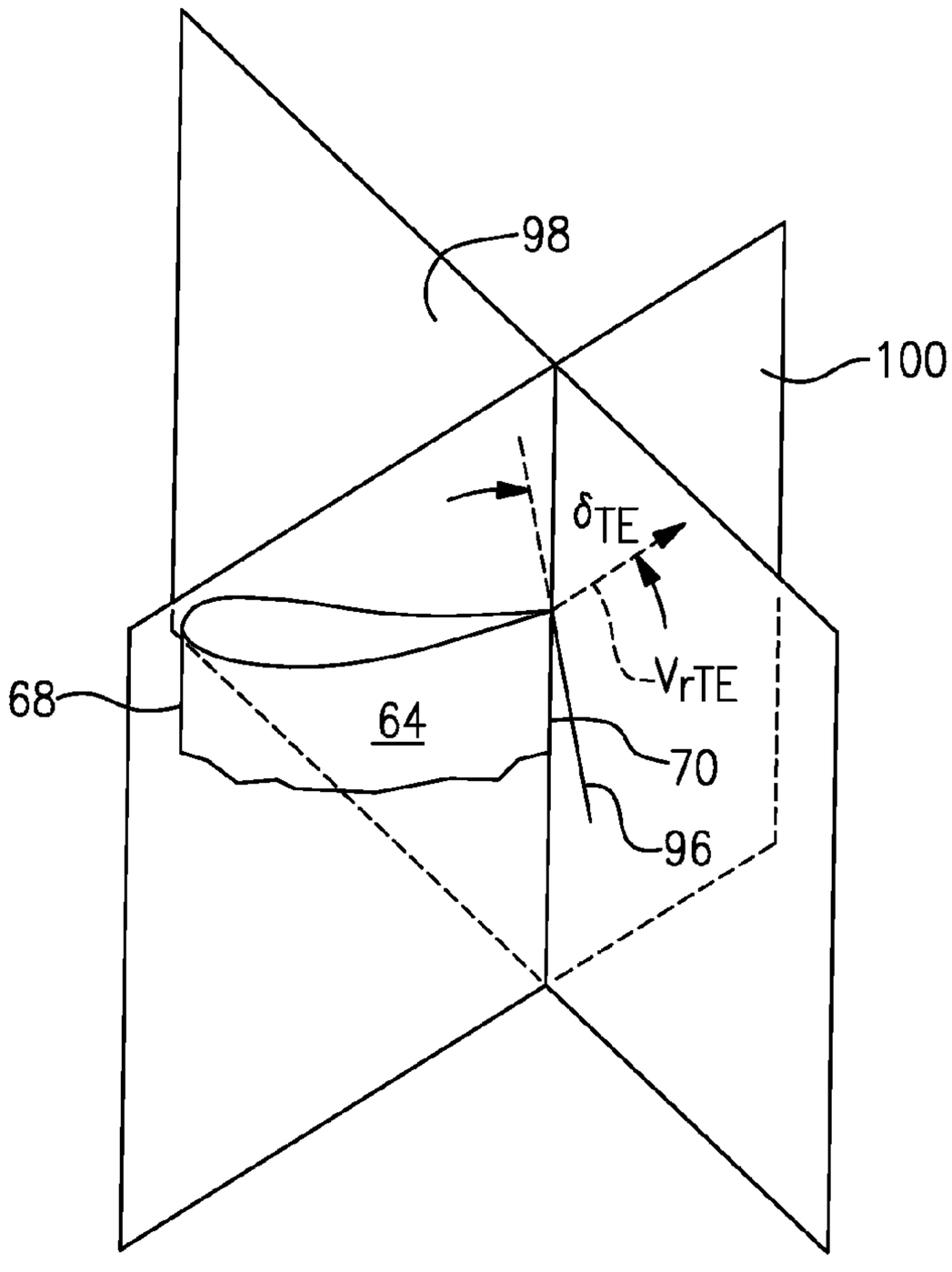

FIG.3D

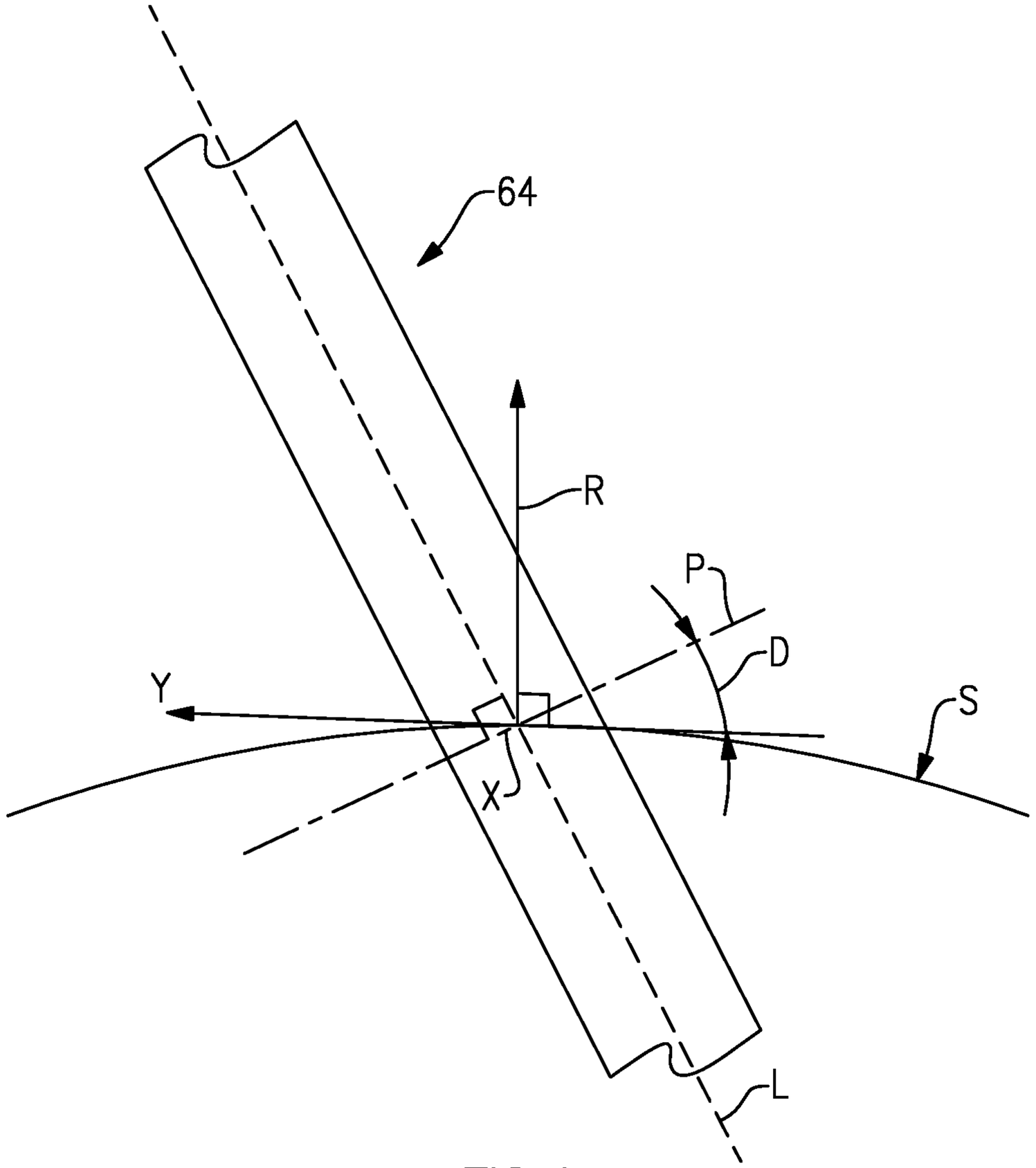

FIG.4

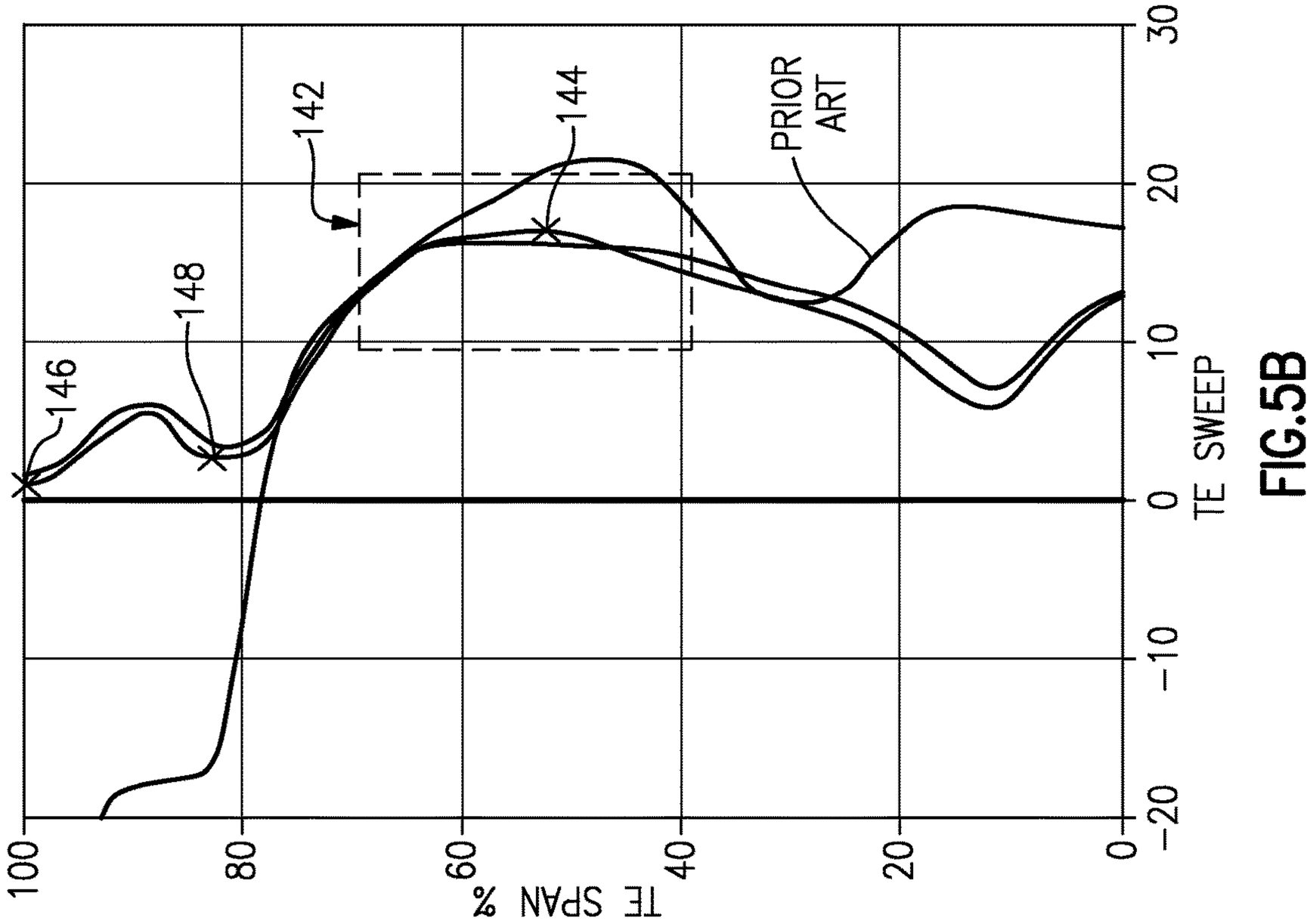
142
144
PRIOR ART
148
146
30
20
10
0
−10
−20
TE SWEEP
100
80
60
40
20
0
TE SPAN %

FIG.5B

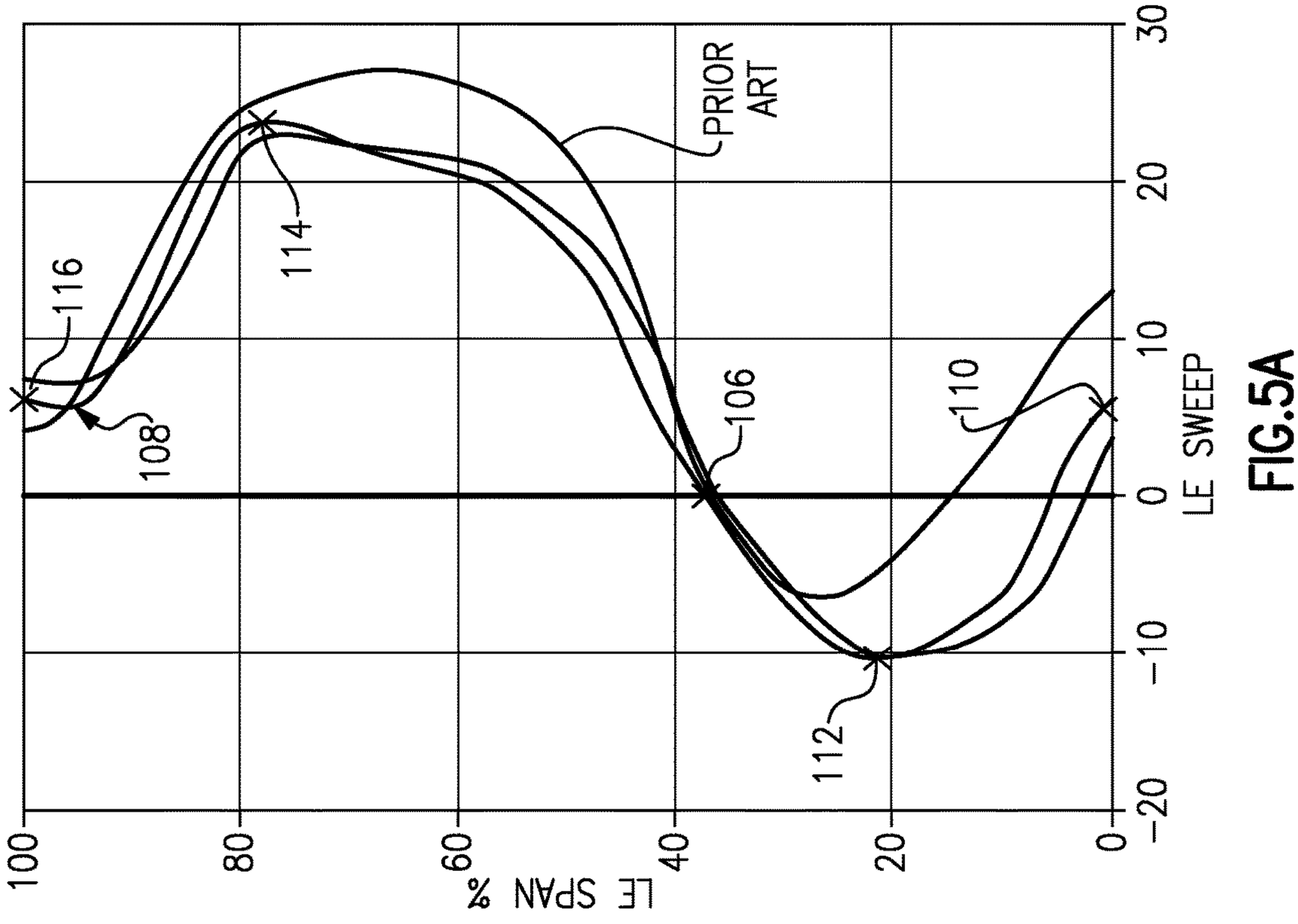
PRIOR ART
114
116
108
106
110
112
30
20
10
0
−10
−20
LE SWEEP
100
80
60
40
20
0
LE SPAN %

FIG.5A

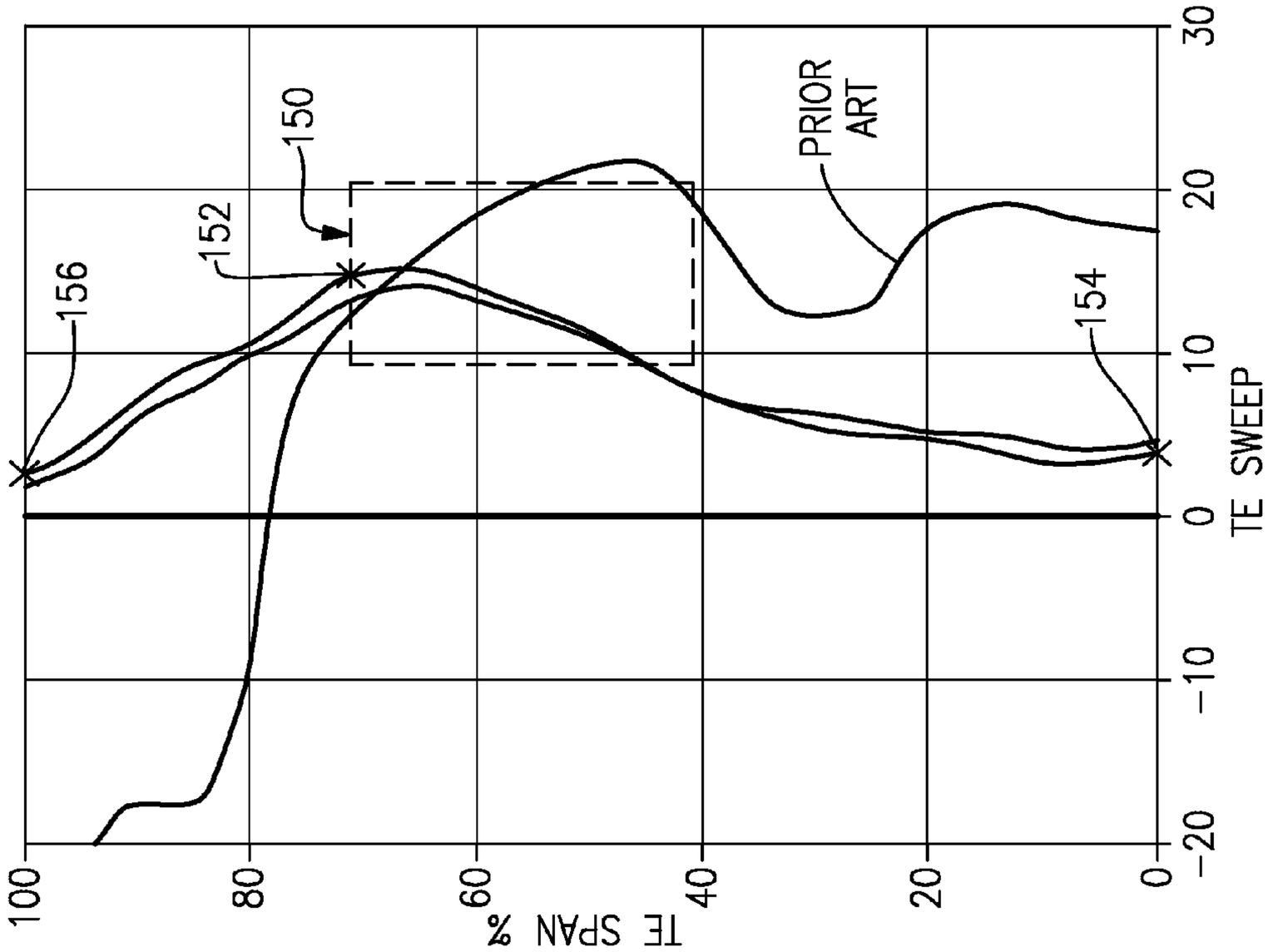
PRIOR ART
150
152
156
154
TE SWEEP
30
20
10
0
−10
−20
100
80
60
40
20
0
TE SPAN %

FIG.6B

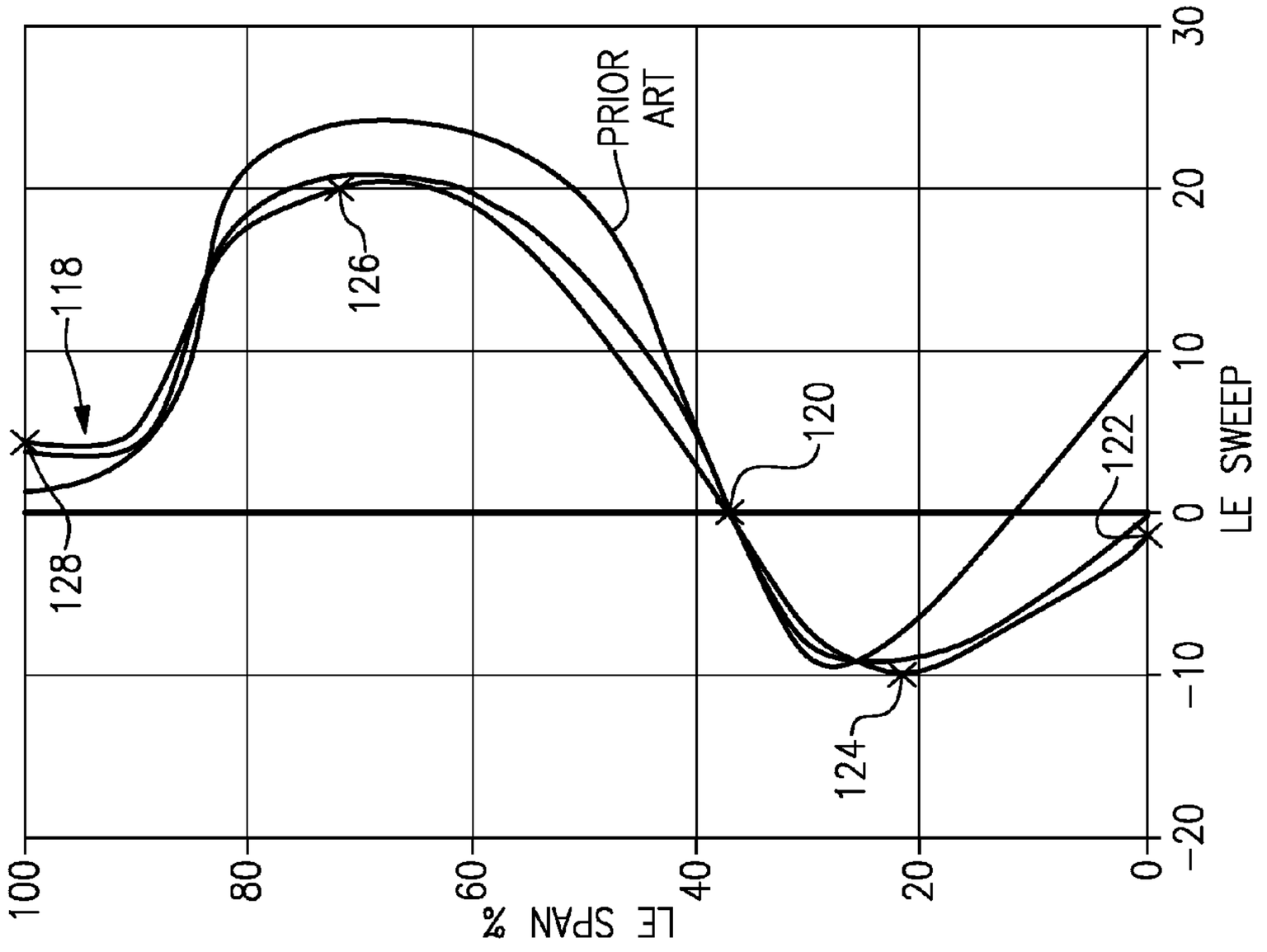
PRIOR ART
118
126
128
120
122
124
LE SWEEP
30
20
10
0
−10
−20
100
80
60
40
20
0
LE SPAN %

FIG.6A

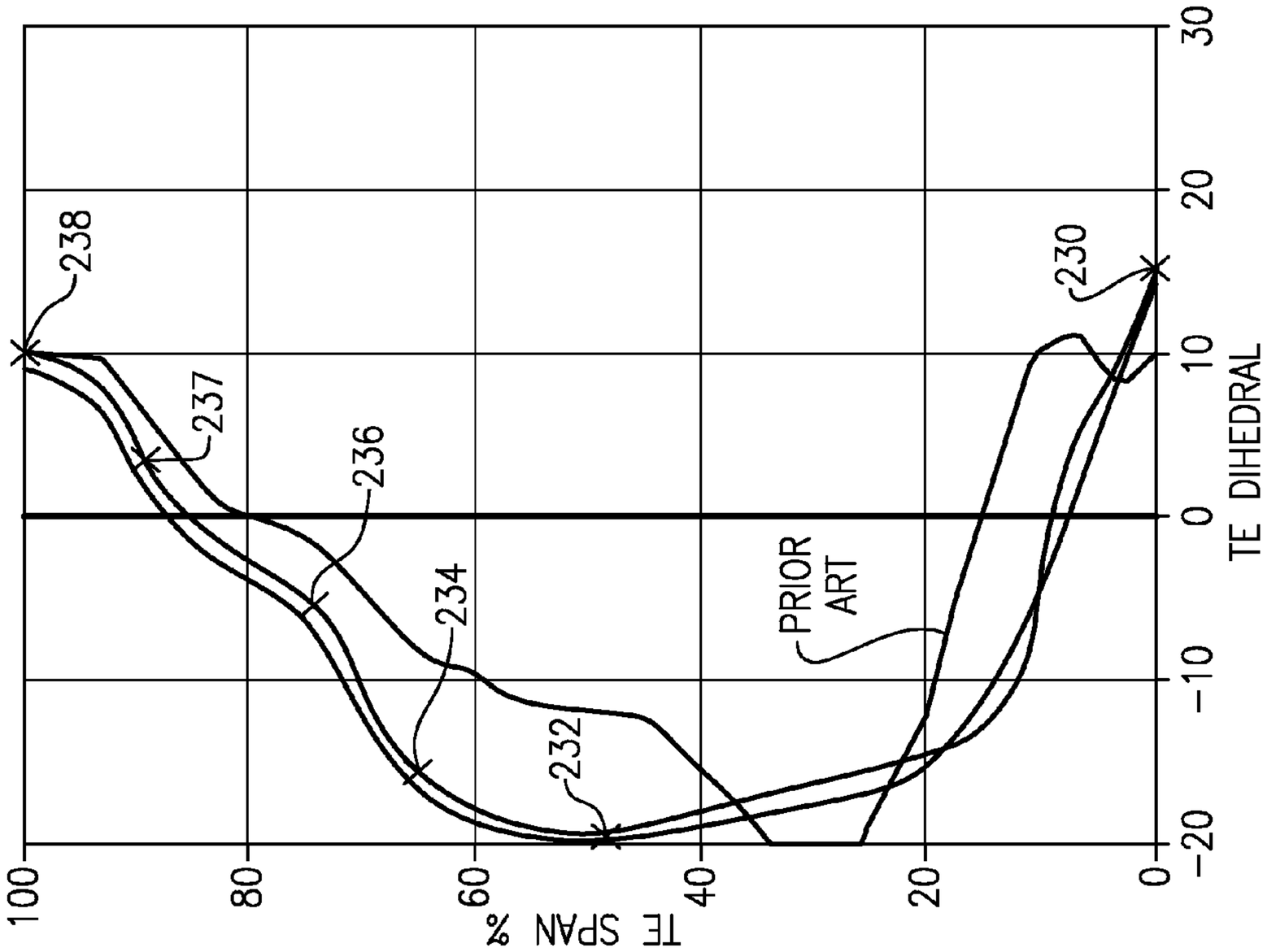
238
237
236
234
232
230
PRIOR ART
TE SPAN %
100
80
60
40
20
0
30
20
10
0
−10
−20
TE DIHEDRAL

FIG.7B

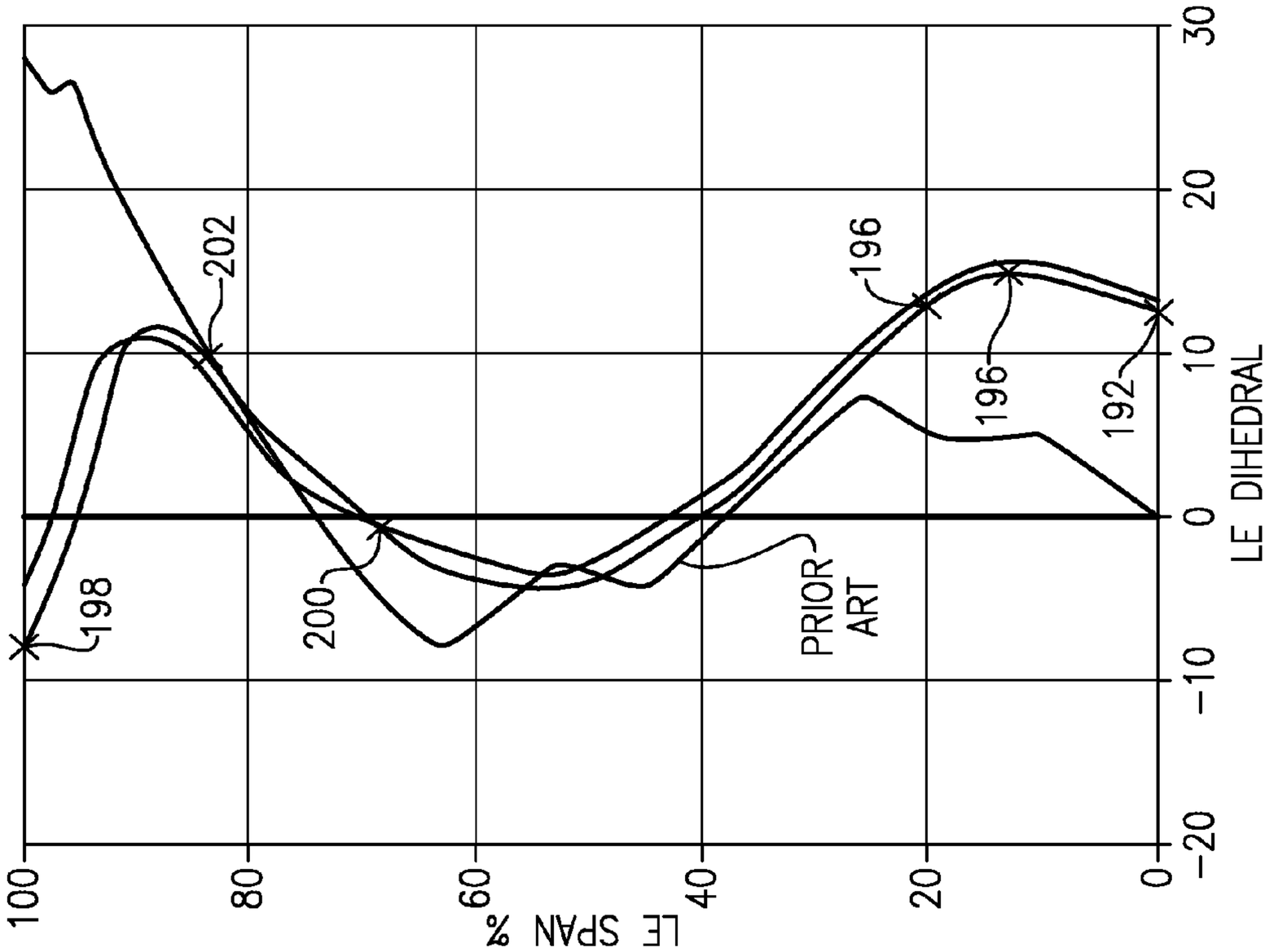
202
198
200
196
192
PRIOR ART
LE SPAN %
100
80
60
40
20
0
30
20
10
0
−10
−20
LE DIHEDRAL

FIG.7A

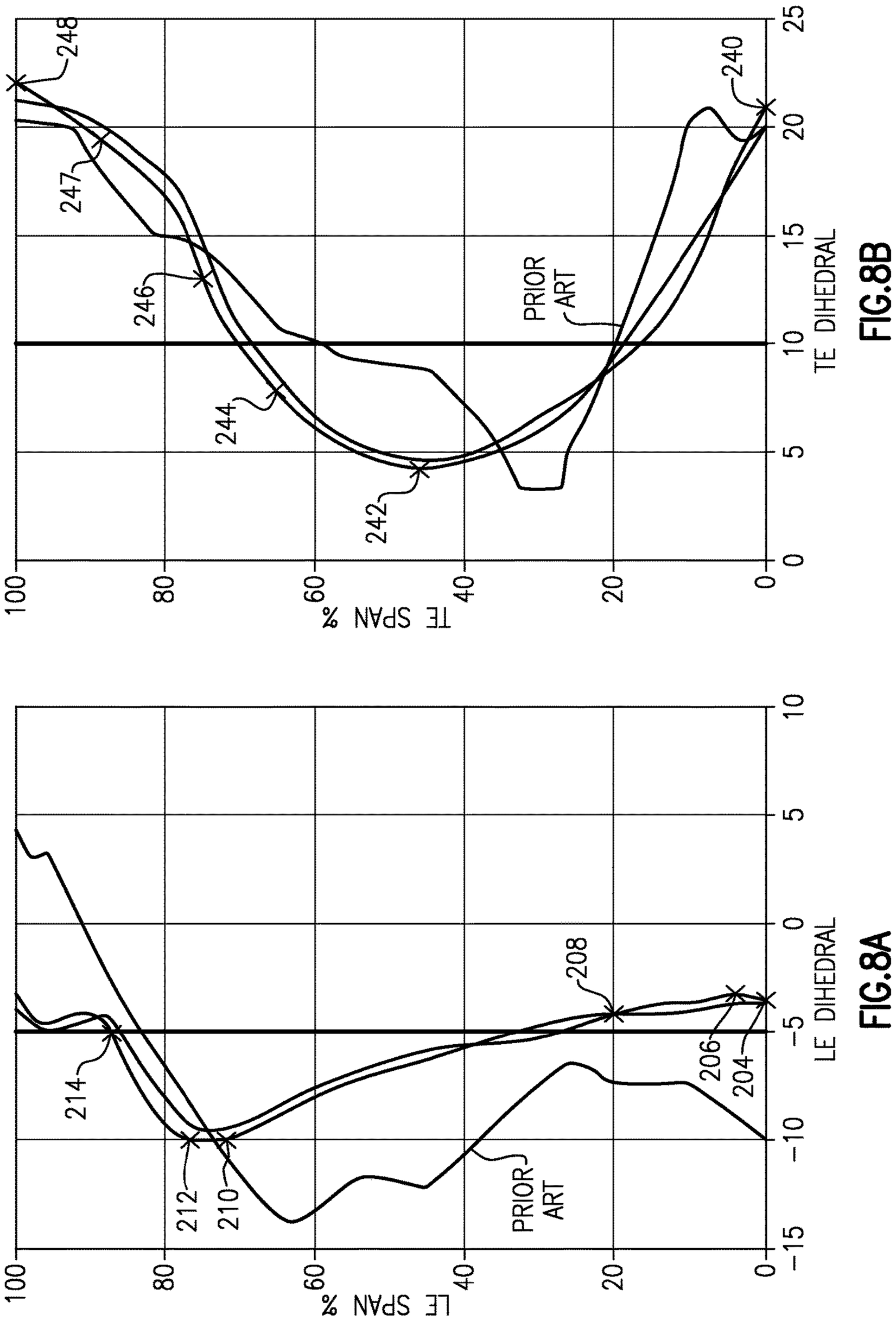
248
247
246
244
242
240
PRIOR ART
25
20
15
10
5
0
TE DIHEDRAL
100
80
60
40
20
0
TE SPAN %

FIG.8B

214
212
210
208
206
204
PRIOR ART
10
5
0
−5
−10
−15
LE DIHEDRAL
100
80
60
40
20
0
LE SPAN %

FIG.8A

GAS TURBINE ENGINE AIRFOIL

CROSS-REFERENCE TO RELATED APPLICATIONS

This application claims priority to U.S. Provisional Application No. 61/942,026, which was filed on Feb. 19, 2014 and is incorporated herein by reference.

BACKGROUND

This disclosure relates generally to an airfoil for gas turbine engines, and more particularly to a fan or compressor blade and the relationship between the blade's aerodynamic leading edge sweep and aerodynamic leading edge dihedral.

A turbine engine such as a gas turbine engine typically includes a fan section, a compressor section, a combustor section and a turbine section. Air entering the compressor section is compressed and delivered into the combustor section where it is mixed with fuel and ignited to generate a high-speed exhaust gas flow. The high-speed exhaust gas flow expands through the turbine section to drive the compressor and the fan section. The compressor section typically includes low and high pressure compressors, and the turbine section includes low and high pressure turbines.

The propulsive efficiency of a gas turbine engine depends on many different factors, such as the design of the engine and the resulting performance debits on the fan that propels the engine. As an example, the fan may rotate at a high rate of speed such that air passes over the fan airfoils at transonic or supersonic speeds. The fast-moving air creates flow discontinuities or shocks that result in irreversible propulsive losses. Additionally, physical interaction between the fan and the air causes downstream turbulence and further losses. Although some basic principles behind such losses are understood, identifying and changing appropriate design factors to reduce such losses for a given engine architecture has proven to be a complex and elusive task.

SUMMARY

In one exemplary embodiment, an airfoil for a turbine engine includes an airfoil that has pressure and suction sides that extend in a radial direction from a 0% span position at an inner flow path location to a 100% span position at an airfoil tip. The airfoil has a curve that corresponds to a relationship between a trailing edge sweep angle and a span position. The trailing edge sweep angle is in a range of 10° to 20° in a range of 40-70% span position, and the trailing edge sweep angle is positive from 0% span to at least 95% span. The airfoil has a relationship between a leading edge dihedral and a span position. The leading edge dihedral is negative from the 0% span position to the 100% span position. A positive dihedral corresponds to suction side-leaning, and a negative dihedral corresponds to pressure side-leaning.

In a further embodiment of the above, the trailing edge sweep angle is in a range of 10° to 20° in a range of 50-70% span position.

In a further embodiment of any of the above, the trailing edge sweep angle is in a range of 10° to 20° in a range of 60-70% span position.

In a further embodiment of any of the above, the trailing edge sweep angle is positive from 0%-95% span.

In a further embodiment of any of the above, the trailing edge sweep angle transitions from less positive to more positive at greater than an 80% span position.

In a further embodiment of any of the above, a positive-most trailing edge sweep angle is at a greater than 50% span position.

In a further embodiment of any of the above, a positive-most trailing edge sweep angle is at about a 70% span position.

In a further embodiment of any of the above, a trailing edge sweep angle is within 5° along a portion of the curve from the 0% span position to a 60% span position.

In a further embodiment of any of the above, a positive-most trailing edge sweep angle lies along the portion.

In a further embodiment of any of the above, a positive-most trailing edge sweep angle is within the range of 10° to 20° in the range of 40-70% span position.

In a further embodiment of any of the above, the airfoil has a leading edge sweep angle curve that corresponds to a relationship between a leading edge sweep angle and a span position. A leading edge sweep angle at the 100% span position is less negative than a forward-most leading edge sweep angle along the curve. The curve has a decreasing leading edge sweep angle rate in a range of a 80-100% span position.

In a further embodiment of any of the above, the leading edge sweep angle curve has a portion that extends span-wise toward the tip and from the forward-most leading edge sweep angle. The portion has a decreasing leading edge sweep angle that crosses a zero sweep angle in the range of a 30-40% span position.

In a further embodiment of any of the above, the forward-most leading edge sweep angle is in a range of −10° to −15°.

In a further embodiment of any of the above, the forward-most leading edge sweep angle is about −10°.

In a further embodiment of any of the above, a rearward-most leading edge sweep angle is in a range of 15° to 30°.

In a further embodiment of any of the above, a leading edge sweep angle at the 0% span position and a leading edge sweep angle at the 100% span position are within 5° of one another.

In a further embodiment of any of the above, a leading edge sweep angle at the 0% span position is negative, and a leading edge sweep angle at the 100% span position is positive.

In a further embodiment of any of the above, the leading edge sweep angle at the 0% span position is positive. The leading edge sweep angle at the 100% span position is negative.

In a further embodiment of any of the above, the leading edge dihedral at the 0% span position is in the range of −3° to −12°.

In a further embodiment of any of the above, the leading edge dihedral at the 0% span position is about −4°.

In a further embodiment of any of the above, the leading edge dihedral at the 0% span position is about −10°.

In a further embodiment of any of the above, the leading edge dihedral extends from the 0% span position to a 20% span position and has a leading edge dihedral in a range of −2° to −6°.

In a further embodiment of any of the above, the leading edge dihedral includes a first point at a 75% span position and extends generally linearly from the first point to a second point at the 85% span position.

In a further embodiment of any of the above, a maximum negative dihedral is in a range of 95-100% span position.

In a further embodiment of any of the above, a least negative dihedral is in a range of 5-15% span position.

In a further embodiment of any of the above, a maximum negative dihedral is in a range of 65-75% span position.

In a further embodiment of any of the above, a least negative dihedral is in a range of 0-10% span position.

In a further embodiment of any of the above, a maximum negative dihedral is in a range of 50-60% span position.

In a further embodiment of any of the above, the airfoil is a fan blade for a gas turbine engine.

In a further embodiment of any of the above, the airfoil has a relationship between a trailing edge dihedral and a span position. The trailing edge dihedral is positive from the 0% span position to the 100% span position. A positive dihedral corresponds to suction side-leaning and a negative dihedral corresponds to pressure side-leaning.

BRIEF DESCRIPTION OF THE DRAWINGS

The disclosure can be further understood by reference to the following detailed description when considered in connection with the accompanying drawings wherein:

FIG. **1** schematically illustrates a gas turbine engine embodiment.

FIG. **2**A is a perspective view of a portion of a fan section.

FIG. **2**B is a schematic cross-sectional view of the fan section.

FIG. **2**C is a cross-sectional view a fan blade taken along line **2**C-**2**C in FIG. **2**B.

FIG. **3**A is a schematic view of fan blade span positions for an airfoil without any curvature at the leading and trailing edges.

FIG. **3**B is an elevational view of a fan blade airfoil illustrating velocity vectors in relation to the leading and trailing edges.

FIG. **3**C is a schematic perspective view of an airfoil fragment illustrating the definition of a leading edge sweep angle.

FIG. **3**D is a schematic perspective view of an airfoil fragment illustrating the definition of a trailing edge sweep angle.

FIG. **4** is a schematic representation of a dihedral angle for an airfoil.

FIG. **5**A graphically illustrates a leading edge sweep angle relative to a span position for a set of first example airfoils and a prior art airfoil.

FIG. **5**B graphically illustrates a trailing edge sweep angle relative to a span position for a set of first example airfoils and a prior art airfoil.

FIG. **6**A graphically illustrates a leading edge sweep angle relative to a span position for a set of second example airfoils and the prior art airfoil.

FIG. **6**B graphically illustrates a trailing edge sweep angle relative to a span position for a set of second example airfoils and the prior art airfoil.

FIG. **7**A illustrates a relationship between a leading edge aerodynamic dihedral angle and a span position for the set of first example airfoils and a prior art curve.

FIG. **7**B illustrates a relationship between a trailing edge aerodynamic dihedral angle and a span position for the set of first example airfoils and a prior art curve.

FIG. **8**A illustrates a relationship between a leading edge aerodynamic dihedral angle and a span position for the set of second example airfoils and the prior art curve.

FIG. **8**B illustrates a relationship between a trailing edge aerodynamic dihedral angle and a span position for the set of second example airfoils and the prior art curve.

The embodiments, examples and alternatives of the preceding paragraphs, the claims, or the following description and drawings, including any of their various aspects or respective individual features, may be taken independently or in any combination. Features described in connection with one embodiment are applicable to all embodiments, unless such features are incompatible.

DETAILED DESCRIPTION

FIG. **1** schematically illustrates a gas turbine engine **20**. The gas turbine engine **20** is disclosed herein as a two-spool turbofan that generally incorporates a fan section **22**, a compressor section **24**, a combustor section **26** and a turbine section **28**. Alternative engines might include an augmenter section (not shown) among other systems or features. The fan section **22** drives air along a bypass flow path B in a bypass duct defined within a nacelle **15**, while the compressor section **24** drives air along a core flow path C for compression and communication into the combustor section **26** then expansion through the turbine section **28**. Although depicted as a two-spool turbofan gas turbine engine in the disclosed non-limiting embodiment, it should be understood that the concepts described herein are not limited to use with two-spool turbofans as the teachings may be applied to other types of turbine engines including three-spool architectures. That is, the disclosed airfoils may be used for engine configurations such as, for example, direct fan drives, or two- or three-spool engines with a speed change mechanism coupling the fan with a compressor or a turbine sections.

The exemplary engine **20** generally includes a low speed spool **30** and a high speed spool **32** mounted for rotation about an engine central longitudinal axis X relative to an engine static structure **36** via several bearing systems **38**. It should be understood that various bearing systems **38** at various locations may alternatively or additionally be provided, and the location of bearing systems **38** may be varied as appropriate to the application.

The low speed spool **30** generally includes an inner shaft **40** that interconnects a fan **42**, a first (or low) pressure compressor **44** and a first (or low) pressure turbine **46**. The inner shaft **40** is connected to the fan **42** through a speed change mechanism, which in exemplary gas turbine engine **20** is illustrated as a geared architecture **48** to drive the fan **42** at a lower speed than the low speed spool **30**. The high speed spool **32** includes an outer shaft **50** that interconnects a second (or high) pressure compressor **52** and a second (or high) pressure turbine **54**. A combustor **56** is arranged in exemplary gas turbine **20** between the high pressure compressor **52** and the high pressure turbine **54**. A mid-turbine frame **57** of the engine static structure **36** is arranged generally between the high pressure turbine **54** and the low pressure turbine **46**. The mid-turbine frame **57** further supports bearing systems **38** in the turbine section **28**. The inner shaft **40** and the outer shaft **50** are concentric and rotate via bearing systems **38** about the engine central longitudinal axis X which is collinear with their longitudinal axes.

The core airflow is compressed by the low pressure compressor **44** then the high pressure compressor **52**, mixed and burned with fuel in the combustor **56**, then expanded over the high pressure turbine **54** and low pressure turbine **46**. The mid-turbine frame **57** includes airfoils **59** which are in the core airflow path C. The turbines **46**, **54** rotationally drive the respective low speed spool **30** and high speed spool **32** in response to the expansion. It will be appreciated that each of the positions of the fan section **22**, compressor section **24**, combustor section **26**, turbine section **28**, and fan drive gear system **48** may be varied. For example, gear system **48** may be located aft of combustor section **26** or even aft of turbine section **28**, and fan section **22** may be positioned forward or aft of the location of gear system **48**.

The engine **20** in one example is a high-bypass geared aircraft engine. In a further example, the engine **20** bypass ratio is greater than about six (6), with an example embodiment being greater than about ten (10), the geared architecture **48** is an epicyclic gear train, such as a planetary gear system or other gear system, with a gear reduction ratio of greater than about 2.3 and the low pressure turbine **46** has a pressure ratio that is greater than about five. In one disclosed embodiment, the engine **20** bypass ratio is greater than about ten (10:1), the fan diameter is significantly larger than that of the low pressure compressor **44**, and the low pressure turbine **46** has a pressure ratio that is greater than about five (5:1). Low pressure turbine **46** pressure ratio is pressure measured prior to inlet of low pressure turbine **46** as related to the pressure at the outlet of the low pressure turbine **46** prior to an exhaust nozzle. The geared architecture **48** may be an epicyclic gear train, such as a planetary gear system or other gear system, with a gear reduction ratio of greater than about 2.3:1. It should be understood, however, that the above parameters are only exemplary of one embodiment of a geared architecture engine and that the present invention is applicable to other gas turbine engines including direct drive turbofans.

The example gas turbine engine includes the fan **42** that comprises in one non-limiting embodiment less than about twenty-six (26) fan blades. In another non-limiting embodiment, the fan section **22** includes less than about twenty (20) fan blades. Moreover, in one disclosed embodiment the low pressure turbine **46** includes no more than about six (6) turbine rotors schematically indicated at **34**. In another non-limiting example embodiment the low pressure turbine **46** includes about three (3) turbine rotors. A ratio between the number of fan blades **42** and the number of low pressure turbine rotors is between about 3.3 and about 8.6. The example low pressure turbine **46** provides the driving power to rotate the fan section **22** and therefore the relationship between the number of turbine rotors **34** in the low pressure turbine **46** and the number of blades **42** in the fan section **22** disclose an example gas turbine engine **20** with increased power transfer efficiency.

A significant amount of thrust is provided by the bypass flow B due to the high bypass ratio. The fan section **22** of the engine **20** is designed for a particular flight condition—typically cruise at about 0.8 Mach and about 35,000 feet. The flight condition of 0.8 Mach and 35,000 ft, with the engine at its best fuel consumption—also known as "bucket cruise Thrust Specific Fuel Consumption ('TSFCT')"—is the industry standard parameter of lbm of fuel being burned divided by lbf of thrust the engine produces at that minimum point. "Low fan pressure ratio" is the pressure ratio across the fan blade alone, without a Fan Exit Guide Vane ("FEGV") system. The low fan pressure ratio as disclosed herein according to one non-limiting embodiment is less than about 1.55. In another non-limiting embodiment the low fan pressure ratio is less than about 1.45. In another non-limiting embodiment the low fan pressure ratio is from 1.1 to 1.45. "Low corrected fan tip speed" is the actual fan tip speed in ft/sec divided by an industry standard temperature correction of $[(\text{Tram}^\circ\ \text{R})/(518.7^\circ\ \text{R})]^{0.5}$. The "low corrected fan tip speed" as disclosed herein according to another non-limiting embodiment is less than about 1200 ft/second.

Referring to FIG. **2**A-**2**C, the fan blade **42** is supported by a fan hub **60** that is rotatable about the axis X. Each fan blade **42** includes an airfoil **64** extending in a radial span direction R from a root **62** to a tip **66**. A 0% span position corresponds to a section of the airfoil **64** at the inner flow path (e.g., a platform), and a 100% span position corresponds to a section of the airfoil **64** at the tip **66**.

The root **62** is received in a correspondingly shaped slot in the fan hub **60**. The airfoil **64** extends radially outward of the platform, which provides the inner flow path. The platform may be integral with the fan blade or separately secured to the fan hub, for example. A spinner **66** is supported relative to the fan hub **60** to provide an aerodynamic inner flow path into the fan section **22**.

The airfoil **64** has an exterior surface **76** providing a contour that extends from a leading edge **68** aftward in a chord-wise direction H to a trailing edge **70**, as shown in FIG. **2**C. Pressure and suction sides **72**, **74** join one another at the leading and trailing edges **68**, **70** and are spaced apart from one another in an airfoil thickness direction T. An array of the fan blades **42** are positioned about the axis X in a circumferential or tangential direction Y. Any suitable number of fan blades may be used in a given application.

The exterior surface **76** of the airfoil **64** generates lift based upon its geometry and directs flow along the core flow path C. The fan blade **42** may be constructed from a composite material, or an aluminum alloy or titanium alloy, or a combination of one or more of these. Abrasion-resistant coatings or other protective coatings may be applied to the fan blade **42**. The curves and associated values assume a fan in a hot, running condition (typically cruise).

One characteristic of fan blade performance relates to the fan blade's leading and trailing edge sweep angles relative to a particular span position (R direction). Referring to FIG. **3**A, span positions a schematically illustrated from 0% to 100% in 10% increments. Each section at a given span position is provided by a conical cut that corresponds to the shape of the core flow path, as shown by the large dashed lines. In the case of a fan blade with an integral platform, the 0% span position corresponds to the radially innermost location where the airfoil meets the fillet joining the airfoil to the platform. In the case of a fan blade without an integral platform, the 0% span position corresponds to the radially innermost location where the discrete platform meets the exterior surface of the airfoil. In addition to varying with span, leading and trailing edge sweep varies between a hot, running condition and a cold, static ("on the bench") condition.

The axial velocity Vx (FIG. **3**B) of the core flow C is substantially constant across the radius of the flowpath. However the linear velocity U of a rotating airfoil increases with increasing radius. Accordingly, the relative velocity Vr of the working medium at the airfoil leading edge increases with increasing radius, and at high enough rotational speeds, the airfoil experiences supersonic working medium flow velocities in the vicinity of its tip. The relative velocity at the leading edge **68** is indicated as Vr_{LE}, and the relative velocity at the trailing edge **70** is indicated as Vr_{TE}.

Supersonic flow over an airfoil, while beneficial for maximizing the pressurization of the working medium, has the undesirable effect of reducing fan efficiency by introducing losses in the working medium's total pressure. Therefore, it is typical to sweep the airfoil's leading edge over at least a portion of the blade span so that the working medium velocity component in the chordwise direction (perpendicular to the leading edge) is subsonic. Since the relative velocity Vr increases with increasing radius, the sweep angle typically increases with increasing radius as well. As shown in FIGS. **3**C and **3**D, the sweep angle σ at any arbitrary radius Rd (FIG. **3**A) at the leading edge **68** is indicated as σ_{LE}, and at the trailing edge **70**, σ_{TE}.

Referring to FIG. **3**C, the leading edge sweep angle σ_{LE} is the acute angle between a line **90** tangent to the leading edge **68** of the airfoil **64** and a plane **92** perpendicular to the relative velocity vector Vr_{LE}. The sweep angle is measured in plane **94**, which contains both the relative velocity vector Vr_{LE} and the tangent line **90** and is perpendicular to plane **92**. FIGS. **5**A and **6**A are provided in conformance with this definition of the leading edge sweep angle σ_{LE}.

Referring to FIG. **3**D, the trailing edge sweep angle a is the acute angle between a line **96** tangent to the trailing edge **70** of the airfoil **64** and a plane **98** perpendicular to the relative velocity vector Vr_{TE}. The sweep angle is measured in plane **100**, which contains both the relative velocity vector Vr_{TE} and the tangent line **96** and is perpendicular to plane **98**. FIGS. **5**B and **6**B are provided in conformance with this definition of the trailing edge sweep angle σ_{TE}.

Thus, a negative sweep angle indicates an airfoil edge locally oriented in a direction opposite the velocity vector (Vr_{LE} or Vr_{TE}), and a positive sweep angle indicates an airfoil edge locally oriented in the same direction as the velocity vector.

An aerodynamic dihedral angle D (simply referred to as "dihedral") is schematically illustrated in FIG. **4** for a simple airfoil. An axisymmetric stream surface S passes through the airfoil **64** at a location that corresponds to a span location (FIG. **3**A). For the sake of simplicity, the dihedral D relates to the angle at which a line L along the leading or trailing edge tilts with respect to the stream surface S. A plane P is normal to the line L and forms an angle with the tangential direction Y, providing the dihedral D. A positive dihedral D corresponds to the line tilting toward the suction side (suction side-leaning), and a negative dihedral D corresponds to the line tilting toward the pressure side (pressure side-leaning). The method of determining and calculating the dihedral for more complex airfoil geometries is disclosed in Smith Jr., Leroy H., and Yeh, Hsuan "Sweep and Dihedral Effects in Axial-Flow Turbomachinery." *J. Basic Eng.* Vol. 85 Iss. 3, pp. 401-414 (Sep. 1, 1963), which is incorporated by reference in its entirety. Leading and trailing edge dihedral, like sweep, varies between a hot, running condition and a cold, static ("on the bench") condition.

Several example fan blades are shown in each of the graphs in FIGS. **5**A-**6**B, each blade represented by a curve. Only one curve in each graph is discussed for simplicity. Referring to FIGS. **5**A and **6**A, the airfoil has a curve corresponding to a relationship between a leading edge sweep angle (LE SWEEP) and a span position (LE SPAN %). The curves illustrate that a leading edge sweep angle at the 100% span position (**116** in FIG. **5**A; **128** in FIG. **6**A) is less negative than a forward-most leading edge sweep angle (**112** in FIG. **5**A; **124** in FIG. **6**A) along the curve. The curves have a decreasing leading edge sweep angle rate (**108** in FIG. **5**A; **118** in FIG. **6**A) in a range of a 80-100% span position. That is, the sweep angle is not constant, but changes. This change, or leading edge sweep angle rate, decreases in the range of 80-100% span.

The curves have a portion extending span-wise toward the tip and from the forward-most leading edge sweep angle (**112** in FIG. **5**A; **124** in FIG. **6**A). The forward-most leading edge sweep angle is in a range of −10° to −15°. In the examples shown in FIGS. **5**A and **6**A, the forward-most leading edge sweep angle is about −10°. The portion has a decreasing leading edge sweep angle that crosses a zero sweep angle (**106** in FIG. **5**A; **120** in FIG. **6**A) in the range of a 30-40% span position.

A rearward-most leading edge sweep angle (**114** in FIG. **5**A; **126** in FIG. **6**A) is in a range of 15° to 30°. In the example shown in FIG. **5**A, the rearward-most leading edge sweep angle **114** is in a range of 75-85% span position. With continuing reference to FIG. **5**A, a leading edge sweep angle **110** at the 0% span position and the leading edge sweep angle **116** at the 100% span position are within 5° of one another. Both the leading edge sweep angle at the 0% span position and the leading edge sweep angle at the 100% span position are positive.

Referring to FIG. **6**A, a leading edge sweep angle **122** at the 0% span position is negative, and a leading edge sweep angle **128** at the 100% span position is positive. The leading edge sweep angle **128** at the 0% span position and the leading edge sweep angle **128** at the 100% span position are within 10° of one another.

Trailing edge sweep angles are graphically illustrated in FIGS. **5**B and **6**B. The airfoil has curves corresponding to a relationship between a trailing edge sweep angle and the span position. Within a region of the curve (**142** in FIG. **5**B; **150** in FIG. **6**B), the trailing edge sweep angle (TE SWEEP) is in a range of 10° to 20° in a range of 40-70% span position (TE SPAN %). The trailing edge sweep angle is positive from 0% span to at least 95% span. In one example, the trailing edge sweep angle is in a range of 10° to 20° in a range of 50-70% span position, and in another example, the trailing edge sweep angle is in a range of 10° to 20° in a range of 60-70% span position. Within the 60-70% span position, the trailing edge sweep angle is about 15°. In the examples, a positive-most trailing edge sweep angle (**144** in FIG. **5**B; **152** in FIG. **6**B) is within the range of 10° to 20° in the range of 40-70% span position.

Referring to FIG. **5**B, the trailing edge sweep angle is positive from 0%-95% span. The trailing edge sweep angle **146** at the 100% span position is about zero, but negative. The trailing edge sweep angle transitions from less positive to more positive at greater than an 80% span position at point **148**. The positive-most trailing edge sweep angle **144** is at a greater than 50% span position.

Referring to FIG. **5**B, a trailing edge sweep angle **154** at the 0% span position and a trailing edge sweep angle **156** at the 100% span position are about the same. The positive-most trailing edge sweep angle **152** is at about a 70% span position.

The leading and trailing edge sweep in a hot, running condition along the span of the airfoils **64** relate to the contour of the airfoil and provide necessary fan operation in cruise at the lower, preferential speeds enabled by the geared architecture **48** in order to enhance aerodynamic functionality and thermal efficiency. As used herein, the hot, running condition is the condition during cruise of the gas turbine engine **20**. For example, the leading and trailing edge sweep in the hot, running condition can be determined in a known manner using numerical analysis, such as finite element analysis. Example relationships between the leading edge dihedral (LE DIHEDRAL) and the span position (LE SPAN %) are shown in FIGS. **7**A and **8**A for several example fan blades, each represented by a curve. Only one curve in each graph is discussed for simplicity. In the examples, the leading edge dihedral is negative from the 0% span position to the 100% span position.

The leading edge dihedral at the 0% span position (**192** in FIG. **7**A; **204** in FIG. **8**A) is in the range of −3° to −12°. In the examples shown in FIGS. **7**A and **8**A, the leading edge dihedral at the 0% span position is about −4°.

The leading edge dihedral extends from the 0% span position to a 20% span position (**196** in FIG. **7**A; **208** in FIG. **8**A) having a leading edge dihedral in a range of −2° to −6°.

In the examples shown in FIGS. **7**A and **8**A, the leading edge dihedral includes a first point (**200** in FIG. **7**A; **210** in FIG. **8**A) at a 75% span position and extends generally linearly from the first point to a second point (**202** in FIG. **7**A; **214** in FIG. **8**A) at the 85% span position. The first point is in a range of −8° to −10° dihedral, and the second point is in a range of −3° to −6° dihedral.

Referring to FIG. **7**A, a maximum negative dihedral **198** is in a range of 95-100% span position. A least negative dihedral **194** is in a range of 5-15% span position. Referring to FIG. **8**A, a maximum negative dihedral **210** is in a range of 65-75% span position. A least negative dihedral **206** is in a range of 0-10% span position.

Example relationships between the trailing edge dihedral and the span position are shown in FIGS. **7**B and **8**B for several example fan blades, each represented by a curve. Only one curve in each graph is discussed for simplicity. In the examples, the trailing edge dihedral is positive from the 0% span position to the 100% span position. The relationship provides a generally C-shaped curve from the 0% span position to a 50% span position and then a 90% span position.

A trailing edge dihedral (**230** in FIG. **7**B; **240** in FIG. **8**B) at the 0% span position is in a range of 20° to 25°. A trailing edge dihedral (**232** in FIG. **7**B; **242** in FIG. **8**B) at about the 50% span position is in a range of 2° to 6°. A trailing edge dihedral (**237** in FIG. **7**B; **247** in FIG. **8**B) at the 90% span position is in a range of 16° to 22°. From a 65% span position (**234** in FIG. **7**B; **244** in FIG. **8**B) to a 75% span position (**236** in FIG. **7**B; **246** in FIG. **8**B) the trailing edge dihedral increases about 5°.

A positive-most trailing edge dihedral (**238** in FIG. **7**B; **248** in FIG. **8**B) in a 80%-100% span position is within 5° of the trailing edge dihedral in the 0% span position (**230** in FIG. **7**B; **240** in FIG. **8**B). A least positive trailing edge dihedral (**232** in FIG. **7**B; **242** in FIG. **8**B) is in a 40%-55% span position.

The leading and trailing edge aerodynamic dihedral angle in a hot, running condition along the span of the airfoils **64** relate to the contour of the airfoil and provide necessary fan operation in cruise at the lower, preferential speeds enabled by the geared architecture **48** in order to enhance aerodynamic functionality and thermal efficiency. As used herein, the hot, running condition is the condition during cruise of the gas turbine engine **20**. For example, the leading and trailing edge aerodynamic dihedral angle in the hot, running condition can be determined in a known manner using numerical analysis, such as finite element analysis. It should also be understood that although a particular component arrangement is disclosed in the illustrated embodiment, other arrangements will benefit herefrom. Although particular step sequences are shown, described, and claimed, it should be understood that steps may be performed in any order, separated or combined unless otherwise indicated and will still benefit from the present invention.

Although the different examples have specific components shown in the illustrations, embodiments of this invention are not limited to those particular combinations. It is possible to use some of the components or features from one of the examples in combination with features or components from another one of the examples.

Although an example embodiment has been disclosed, a worker of ordinary skill in this art would recognize that certain modifications would come within the scope of the claims. For that reason, the following claims should be studied to determine their true scope and content.

What is claimed is:

1. An airfoil for a turbine engine comprising:

an airfoil having pressure and suction sides extending in a radial direction from a 0% span position at an inner flow path location to a 100% span position at an airfoil tip, wherein the airfoil has a curve corresponding to a relationship between a trailing edge sweep angle and a span position, wherein the trailing edge sweep angle is in a range of 10° to 20° in a range of 40-70% span position, and the trailing edge sweep angle is positive from 0% span to at least 95% span, wherein the airfoil has a relationship between a leading edge dihedral and a span position, the leading edge dihedral negative from the 0% span position to the 100% span position, wherein a positive dihedral corresponds to suction side-leaning, and a negative dihedral corresponds to pressure side-leaning.

2. The airfoil according to claim **1**, wherein the trailing edge sweep angle is in a range of 10° to 20° in a range of 50-70% span position.

3. The airfoil according to claim **2**, wherein the trailing edge sweep angle is in a range of 10° to 20° in a range of 60-70% span position.

4. The airfoil according to claim **1**, wherein the trailing edge sweep angle is positive from 0%-95% span.

5. The airfoil according to claim **4**, wherein the trailing edge sweep angle transitions from less positive to more positive at greater than an 80% span position.

6. The airfoil according to claim **4**, wherein a positive-most trailing edge sweep angle is at a greater than 50% span position.

7. The airfoil according to claim **1**, wherein a positive-most trailing edge sweep angle is at about a 70% span position.

8. The airfoil according to claim **1**, wherein a trailing edge sweep angle is within 5° along a portion of the curve from the 0% span position to a 60% span position.

9. The airfoil according to claim **8**, wherein a positive-most trailing edge sweep angle lies along the portion.

10. The airfoil according to claim **1**, wherein a positive-most trailing edge sweep angle is within the range of 10° to 20° in the range of 40-70% span position.

11. The airfoil according to claim **1**, wherein the airfoil has a leading edge sweep angle curve corresponding to a relationship between a leading edge sweep angle and a span position, wherein a leading edge sweep angle at the 100% span position is less negative than a forward-most leading edge sweep angle along the curve, and wherein the curve has a decreasing leading edge sweep angle rate in a range of a 80-100% span position.

12. The airfoil according to claim **11**, wherein the leading edge sweep angle curve has a portion extending span-wise toward the tip and from the forward-most leading edge sweep angle, the portion has a decreasing leading edge sweep angle that crosses a zero sweep angle in the range of a 30-40% span position.

13. The airfoil according to claim **12**, wherein the forward-most leading edge sweep angle is in a range of −10° to −15°.

14. The airfoil according to claim **13**, wherein the forward-most leading edge sweep angle is about −10°.

15. The airfoil according to claim **13**, wherein a rearward-most leading edge sweep angle is in a range of 15° to 30°.

16. The airfoil according to claim **13**, wherein a leading edge sweep angle at the 0% span position and a leading edge sweep angle at the 100% span position are within 5° of one another.

17. The airfoil according to claim 13, wherein a leading edge sweep angle at the 0% span position is negative, and a leading edge sweep angle at the 100% span position is positive.

18. The airfoil according to claim 13, wherein a leading edge sweep angle at the 0% span position is positive, and a leading edge sweep angle at the 100% span position is negative.

19. The airfoil according to claim 1, wherein the leading edge dihedral at the 0% span position is in the range of −3° to −12°.

20. The airfoil according to claim 19, wherein the leading edge dihedral at the 0% span position is about −4°.

21. The airfoil according to claim 2, wherein the leading edge dihedral at the 0% span position is about −10°.

22. The airfoil according to claim 19, wherein the leading edge dihedral extends from the 0% span position to a 20% span position having a leading edge dihedral in a range of −2° to −6°.

23. The airfoil according to claim 22, wherein the leading edge dihedral includes a first point at a 75% span position and extends generally linearly from the first point to a second point at the 85% span position.

24. The airfoil according to claim 19, wherein a maximum negative dihedral is in a range of 95-100% span position.

25. The airfoil according to claim 24, wherein a least negative dihedral is in a range of 5-15% span position.

26. The airfoil according to claim 19, wherein a maximum negative dihedral is in a range of 65-75% span position.

27. The airfoil according to claim 26, wherein a least negative dihedral is in a range of 0-10% span position.

28. The airfoil according to claim 19, wherein a maximum negative dihedral is in a range of 50-60% span position.

29. The airfoil according to claim 1, wherein the airfoil is a fan blade for a gas turbine engine.

30. The airfoil according to claim 1, wherein the airfoil has a relationship between a trailing edge dihedral and a span position, the trailing edge dihedral positive from the 0% span position to the 100% span position, wherein a positive dihedral corresponds to suction side-leaning, and a negative dihedral corresponds to pressure side-leaning.

* * * * *